CONSEQUENCE OF MMP-9 DEFICIENCY ON IOP REGULATION AND RGC SURVIVAL

CONSEQUENCE OF MMP-9 DEFICIENCY ON INTRAOCULAR PRESSURE REGULATION AND RETINAL GANGLION CELL SURVIVAL

By
Anuja Siwakoti, Honours B. Sc.

A Thesis
Submitted to the School of Graduate Studies
in Partial Fulfillment of the Requirements
for the Degree
Master of Science

McMaster University

MASTER OF SCIENCE (2014) McMaster University
(Medical Sciences) Hamilton, Ontario

TITLE: Consequence of MMP-9 deficiency on intraocular pressure regulation and retinal ganglion cell survival
AUTHOR: Anuja Siwakoti, Honours B.Sc.
SUPERVISOR: Dr. Judith West-Mays
NUMBER OF PAGES: x, 66

ABSTRACT

Matrix metalloproteinases (MMPs) are known to be the mediators of extracellular matrix remodeling. Increased levels of matrix metalloproteinases, particularly MMP-9, have been found in the aqueous humor of patients with glaucoma. However the exact role of MMP-9 in glaucomatous changes is not understood. Previous results from the West-Mays' lab indicated that MMP-9 deficient (knockout - KO) mice exhibit elevated IOP, in the absence of distinct morphological changes in the anterior chamber.

In the current thesis, I investigated whether the elevated IOP in MMP-9KO mice leads to RGC death. Wild type and KO littermates at different age groups: 2-3 months, 3-4 months, 6-8 and 9-12 months were studied. IOP was measured using TonoLab rebound tonometer. My results demonstrated that IOP was significantly increased in MMP-9KO mice compared to control littermates at all ages examined. To investigate if the elevated IOP was due to a difference in central corneal thickness (CCT), CCT measurements were made between WT and KO mice using ultrasound pachymeter. There was no difference in CCT demonstrating that the elevated IOP observed in MMP-9KO mice was not related to changes in corneal thickness. To determine whether the elevated IOP led to RGC death, the animals were sacrificed, eyes were enucleated and retinas (n=4) from both WT and KO animals were dissected and stained with Brn-3a antibody. Additional eyes were harvested from both WT and KO mice for histological and immunofluorescence studies. I found no observable difference in $Brn3a^+$ RGC count between MMP9-WT and KO mice. Furthermore, no difference in retinal morphology, glial reactivity and laminin expression between WT and KO mice was observed. In the future it will be important to investigate whether elevated IOP in the MMP-9KO mice leads to optic nerve axonal loss and further investigate the possibility that the MMP-9KO retina is neuroprotected.

ACKNOWLEDGEMENTS

My interest in vision science sparked during a volunteer trip to Nepal in 2011. It was at this time that I realized I knew very little about the eyes and it was through this experience that I solidified my desire to be involved in vision research. I am indebted to my supervisor Dr. Judy West-Mays for providing me with an opportunity to gain valuable vision research experience in her lab. Thank you Judy for training me to be a thoughtful scientist. I appreciate all of the advice and guidance you provided to me throughout these two years. I am really impressed by your work-life balance and I am truly thankful to you for allowing me to present my research at various local and international vision research conferences.

I would like to thank my thesis committee members Dr. Alexander Ball and Dr. Amadeo Rodriguez. I could not have asked for a better committee. Your input greatly shaped how I think as a scientist and your kindness and support have been invaluable. Thank you Dr. Ball for helping me with my bench work and for always being there to answer any questions regarding my research. Thank you Dr. Rodriguez for sharing your clinical expertise and for promptly replying to my emails despite your busy schedule.

An ideal job is one where you look forward to coming to the workplace every day. However, this would have been impossible without the support and friendship of wonderful colleagues. I would like to thank the West-Mays' lab members, past and present, including Paula Deschamps, Dr. Jen Robertson, Dr. Christine Kerr, Dr. Aftab Taiyab, Madhuja Gupta, Anna Korol, Scott Bowman, Mizna Zaveri and Vanessa Martino for making the lab so much fun and for making my learning very exciting. Also, thank you Tom, Connie, Mary, Alan and Elyse for your friendship and support. A big thanks goes to Tom for performing optic nerve crush procedures for my project.

I am grateful to Birat and Sachet for their encouragement and support. I could always count on them to cheer me up when I was overwhelmed with academic responsibilities. I would like to thank my family in Nepal for their love, support and encouragement, especially my parents. They see education as the most valuable thing you can give someone, and for that I am truly grateful. Most importantly, I am indebted to my grandmother. From an early age, she made everything seem possible to me. To her, I dedicate this thesis.

TABLE OF CONTENTS

LIST OF FIGURES AND TABLES

LIST OF ABBREVIATIONS

ANOVA	analysis of variance
BDNF	brain derived neurotrophic factor
Brn3a	brain-specific homeobox/ POU domain protein 3A
Brn3a+	brain-specific homeobox/ POU domain protein 3A positive cells
CCT	central corneal thickness
CI	confidence interval
DAPI	4', 6-diamidino-2-phenylindole
DMSO	Dimethyl sulfoxide
DNA	Deoxyribonucleic acid
ECM	extracellular matrix
GCL	ganglion cell layer
GFAP	glial fibrillary acidic protein
H&E	hematoxylin and eosin
Iba-1	ionized calcium binding adaptor molecule 1
i.p.	intraperitoneal
ILM	inner limiting membrane
INL	inner nuclear layer
IOP	intraocular pressure
KA	kainic acid
KO	knockout

mm Hg	millimeters of mercury
MMP	matrix metalloproteinase
NDS	normal donkey serum
NMDA	N-methyl-D-aspartate
OHst	hydroxystilbamidine methanesulfonate
ON	optic nerve
ONC	optic nerve crush
ONH	optic nerve head
ONL	outer nuclear layer
ONT	optic nerve transection
PBS	phosphate buffered saline
POU	Pit-Oct-Unc
PPD	paraphenylenediamine
RGC	retinal ganglion cells
RPE	retinal pigment epithelium
TIMP	tissue inhibitor of matrix metalloproteinase
TM	trabecular meshwork
WT	wild type

CHAPTER ONE

GENERAL INTRODUCTION

1.1 The Eye: Structure and Function

The eye is a highly specialized photoreceptive organ, which processes light energy from the environment and converts it into signals that can stimulate the rod and cone cells of the retina. The human eye is spherical in shape and it can be divided into two segments: the anterior segment and the posterior segment. The general anatomy of the eye is shown in Figure 1.

The anterior segment of the eye consists of the cornea, iris, ciliary body and lens (Forrester, 2008). The outermost transparent structure of the anterior segment or the "window" of the eye is the cornea. The cornea is normally avascular and this structure is responsible for about two-thirds of the eye's focusing power (Lens, 2008). The iris forms the colored portion of the eye. The iris sphincter muscle contracts to constrict the pupil and relaxes to dilate the pupil (Smith, 2008). Through dilation and constriction of the iris muscles, the pupil regulates the amount of light sent to the retina and helps to form clear images on the retina. The crystallin lens is attached to the ciliary body by thin fibers called zonules. While the lens has less refractive power (15 diopters) than the cornea, the lens has the ability to change shape, under the influence of the ciliary muscle and this process is known as accommodation (Forrester, 2008). Unfortunately, the ability of the lens to accommodate slowly gets lost, as we grow older.

In a normal eye, aqueous humor is secreted by a layer of epithelial cells in the iris and ciliary body (Goel, Picciani, Lee, & Bhattacharya, 2010). The aqueous humor then flows into the anterior chamber through the pupil around the iris and drains out through the outflow pathway (refer to Figure 2). There are two main aqueous outflow pathways: 1) Conventional or trabecular pathway and 2) Unconventional or uveoscleral pathway.

The conventional pathway of the eye consists of a series of endothelial cell-lined channels in the angle of the anterior chamber: the trabecular meshwork (TM), Schlemm's canal, the collector channels, and the episcleral venous system (Llobet, Gasull, & Gual, 2003). The trabecular meshwork region consists of the uveal meshwork, corneoscleral meshwork, cribriform or juxtacanalicular meshwork, inner endothelial wall and Schlemm's canal (refer to Figure 3). As the intercellular spacing between cells decreases from uveal meshwork to inner wall of Schlemm's canal, resistance to aqueous humor outflow increases. On the other hand, the unconventional pathway consists of drainage through the spaces between ciliary muscle bundles into suprachoroidal space (Lindsey, 2002). From here, aqueous humor drains either towards the choriocapillaris, reaching the blood circulation, or externally, passing through the sclera and conjunctiva towards the lymphatics vessels (Lindsey, 2002).

The posterior segment consists of the vitreous, choroid and retina (Lens, 2008). In a human eye, the vitreous cavity is the largest cavity of the eye (two-thirds the volume of the eye) and contains the vitreous humor. The choroid is rich with blood vessels and provides nourishment for the retina's photoreceptors-rods and cones. The retina is the innermost lining of the posterior segment of the eye and it is a highly specialized part of the brain. There are two basic layers of the retina: the inner neurosensory layer and the outer retinal pigment epithelium (RPE) layer. The neural layer consists of nine layers; from outer to inner they are: photoreceptors, external limiting membrane, outer nuclear layer, outer plexiform layer, inner nuclear layer, inner plexiform layer, ganglion cell layer, nerve fiber layer and internal limiting membrane (Smith, 2008) (refer to Figure 4). Trophic factors, such as brain-derived neurotrophic factor and nerve growth factor, are

essential to the survival of retinal ganglion cells (RGCs) and they are retrogradely transported from the axonal terminals of RGCs to their cell bodies (Weinreb & Khaw, 2004). The RPE layer, however, is a single layer of cells. It is a highly pigmented epithelial cell layer that absorbs excess light and functions for waste removal purposes by shedding the destroyed tips of the photoreceptor cells and by the phagocytosis of the photoreceptor outer segments (Forrester, 2008).

As the light enters the eye, it stimulates the photochemicals (i.e. rhodopsin, opsins) in outer segments of the photoreceptors (rods and cones) and the light signal is transduced to an electrical signal that is relayed to second and third order neurons (i.e. bipolar cells, amacrine cells, ganglion cells) in the retina and an electrical signal is generated. This electrical signal exits the eye via the axons of the retinal ganglion cells (RGCs), which form the optic nerve.

The convergence of the optic nerve axons forms a central depression in the disc, known as the optic cup and the optic nerve exits the eye at lamina cribosa, a series of perforated connective tissue sheets (Fechtner & Weinreb, 1994). The optic nerve terminates in the lateral geniculate nucleus and superior colliculus in the brain for visual perception and integration (Weinreb & Khaw, 2004).

1.2 Glaucoma

Glaucoma is described as a group of optic neuropathies that results in a gradual degeneration of RGCs and their axons (Weinreb & Khaw, 2004). Clinically, glaucoma is characterized by the excavation of the optic nerve head and it results in a progressive loss of the visual field (De Groef, Van Hove, Dekeyster, Stalmans, & Moons, 2014; Kuehn, Fingert, & Kwon, 2005). Elevated intraocular pressure (IOP) is the major risk factor of

glaucoma. Other risk factors that have been consistently reported in the literature include age, race, family history, myopia and central corneal thickness (Chen, Lu, Zhang, & Lu, 2012; Cho & Kee, 2014; Day et al., 2011). Since IOP is thus far, the only modifiable risk factor, protective measures target IOP lowering strategies such IOP lowering eye drops and surgeries. However, glaucomatous damage can progress after IOP lowering and it can also occur with normal IOP (Song & Caprioli, 2014). Furthermore, IOP can also increase without any signs or damage to the visual field (Vass et al., 2007).

1.2.1 Epidemiology

Glaucoma is the second most leading cause of blindness in the world and affects over 66.8 million people worldwide and an estimated 8.4 million people with bilateral blindness (Quigley & Broman, 2006). The prevalence of glaucoma is projected to increase with population growth and the aging of the population, and it is expected that this disease will affect over 80 million people worldwide and result in bilateral blindness in 11.2 million people worldwide by the year 2020 (Quigley & Broman, 2006). Blindness from all forms of glaucoma in the USA itself is estimated to cost in excess of $1.5 billion annually (Weinreb & Khaw, 2004).

Glaucoma can be classified as open angle glaucoma or closed angle glaucoma depending on the anatomy of the angle between the iris and cornea as viewed by gonioscopy. Open-angle glaucoma is also nicknamed as “silent thief of sight” because the disease is asymptomatic until there is a significant vision loss. The 2010 global estimates are that 4.5 million are blind due to open-angle glaucoma and 3.9 million are blind due to closed angle glaucoma (Quigley & Broman, 2006). Interestingly, there is also a link between elevated IOP and open angle glaucoma. In Baltimore Eye Survey of more than

5,000 individuals aged 40 and over in east Baltimore, participants who had a screening IOP greater than 30 mm Hg were over 39 times more likely to have open angle glaucoma compared to individuals with an IOP below 15 mm Hg (Sommer et al., 1991). Indeed, in patients with normal tension glaucoma and asymmetric IOP, the eye with raised lOP tends to have greater visual field loss (Fechtner & Weinreb, 1994). It is also interesting to note that in monkey model of glaucoma induced by experimental IOP elevation, features of optic neuropathy were clinically and histologically indistinguishable from human primary open angle glaucoma cases (Fechtner & Weinreb, 1994; Gaasterland, Tanishima, & Kuwabara, 1978; Quigley & Addicks, 1980). Thus, there is evidence that high IOP can cause optic nerve damage. Therefore, it is important to understand how elevated IOP can lead to optic neuropathy.

1.2.2 Relationship between intraocular pressure and optic nerve damage

One theory for open angle glaucoma is that the deposition of extracellular debris in the trabecular meshwork filter as well as surrounding outflow regions may impede the aqueous outflow pathway, subsequently leading to higher IOP and optic nerve damage (Rönkkö, 2007; Schlotzer-Schrehardt, 2002). However, how this elevated IOP leads to neurodegeneration of the optic nerve is not well understood. In 1858, two independent theories were proposed to explain optic nerve damage in glaucoma (Dreyer & Lipton, 1999). Müller believed that optic nerve damage was due to mechanical trauma exerted by raised intraocular pressure (IOP) at lamina cribosa; von Jaegar suggested that compromise in the vasculature of the optic nerve might have a role in glaucomatous damage (Dreyer & Lipton, 1999). In the 1970s, a new theory suggested that elevated IOP would cause axonal transport disturbances of neurotrophic factor at lamina cribosa in the

optic nerve (Anderson & Hendrickson, 1974; Dreyer & Lipton, 1999; Fechtner & Weinreb, 1994). This would prevent neurotrophins from reaching the soma of RGCs, thus triggering apoptosis of these cells (Quigley et al., 1995). In support of this theory, in an acute experimental model of glaucoma in rats, there was a substantial inhibition of retrograde transport of brain derived neurotrophic factor (BDNF) due to intraocular pressure-induced compression of optic nerve axons at the lamina cribrosa (Quigley et al., 2000). Furthermore, glial cells such as astrocytes and microglia can also be activated by elevated intraocular pressure and they can alter the environment of extracellular matrix around lamina cribosa and create a milieu that can cause detrimental events that underlie axonal loss and death of healthy retinal ganglion cells (Ebneter, Casson, Wood, & Chidlow, 2010; Hernandez, 2000; Pena et al., 2001). Thus it is clear that elevated IOP can cause damage to optic nerve, but what causes increased IOP needs to be clearly identified.

1.2.3. Altering extracellular matrix and IOP regulation

Multiple studies have shown that extracellular matrix (ECM) modulating molecules are important in mediating aqueous outflow facility and maintaining IOP homeostasis. Matrix metalloproteinases (MMPs) are proteolytic enzymes that cleave components of ECM and their role in modulating aqueous outflow facility has been reported before. Indeed when human anterior segment cultures were perfused with MMPs, aqueous outflow facility increased, whereas treatment with endogenous inhibitors of MMP activity by TIMP2 or synthetic MMP inhibitors reduced outflow facility (Alexander, Samples, & Acott, 1998; J. M. Bradley et al., 1998). Furthermore, experimental elevation of pressure in perfusion cultures caused a concomitant increase in

outflow facility that coincided with increased MMP activity and ECM turnover (J. M. B. Bradley et al., 2001). These two lines of evidence argue strongly that MMPs are important in ECM turnover in the trabecular meshwork region and they can potentially modulate IOP by adjusting aqueous outflow facility. Furthermore, in the juxtacanalicular layer of trabecular meshwork in open-angle glaucomatous eyes, protein aggregates known as *sheath-derived plaques* have been found (Tektas & Lutjen-Drecoll, 2009). These aggregates contain several ECM proteins, including elastin, collagen, and various proteoglycans, most of which are substrates of various MMPs (Nelson, Fingleton, Rothenberg, & Matrisian, 2000). This lends additional evidence that perhaps in open angled glaucoma, the role of certain MMPs could be compromised, thus leading to the deposition of such aggregates in the trabecular meshwork region and affecting IOP homeostasis.

1.3 Specific matrix metalloproteinases in glaucoma

MMPs are primarily classified according to their substrate specificity, and include collagenases (MMP-1, -8 and -13), gelatinases (MMP -2 and -9), stromelysins (MMP-3, -10 and -11) and others (Nelson et al., 2000). MMPs contribute to the activation of cytokines, liberation of growth factors from the matrix, balance of extracellular matrix synthesis and degradation as well as regulation of wound healing (Birkedal-Hansen et al., 1993; Vu & Werb, 2000). MMPs are known to have a major role in ocular development, normal physiology and disease (Birkedal-Hansen et al., 1993; Sivak & Fini, 2002). Ocular pathologies associated with MMPs include cataract (West-Mays, 2008), diabetic retinopathy (Kowluru, Zhong, & Santos, 2012), dry eye (De Paiva et al., 2006) , glaucoma (De Groef et al., 2014; Schlotzer-Schrehardt, 2002), among others. The

enzymatic activities of MMPs are inhibited by a family of inhibitors, such as tissue inhibitors of metalloproteinases (TIMPs) (Djafarzadeh et al., 2012).

There are several MMPs that have been associated with glaucomatous changes. Interestingly, MMPs are found to be elevated in the aqueous humor (Maatta et al., 2005), optic nerve head (Agapova, Ricard, Salvador-Silva, & Hernandez, 2001) and chamber angle (Rönkkö, 2007) of glaucoma patients. Some of the most widely studied actions of MMPs are discussed below:

1.3.1 MMP-3

The action of MMP-3 in glaucomatous changes seems to be mostly in the posterior segment of the eye. A comparison of mRNA levels between retinas of eyes subjected to unilateral episcleral vein injection of hypertonic saline and contralateral healthy retinas revealed that MMP-3 mRNA increased by 3.5-fold at 35 days post induction of ocular hypertension (Ahmed et al., 2004). Similarly, after optic nerve crush and optic nerve transection, MMP-3 mRNA levels were strongly elevated (i.e., over 50-fold and over 250-fold, respectively) (Agudo et al., 2008; De Groef et al., 2014). These studies demonstrate that MMP-3 may be an important player in the glaucomatous process, at the level of the retina.

1.3.2 MMP-2

In glaucomatous dogs, it has been shown that there is an increase in latent MMP-2 in aqueous humor samples and an increase in active MMP-2 in iridocorneal angle tissue compared to contralateral healthy eyes (Weinstein et al., 2007). Furthermore, in response to IOP elevation, it has been shown that trabecular meshwork cells sense increased mechanical stretching and respond by upregulating their secretion of MMP-2 among

other MMPs (J. M. B. Bradley, Kelley, Rose, & Acott, 2003; J. M. B. Bradley et al., 2001; Vittitow & Borras, 2004; WuDunn, 2001).

In a rat model of experimental glaucoma, MMP-2 increased by 2-fold in the optic nerve head as shown by microarray analysis (Johnson, Jia, Cepurna, Doser, & Morrison, 2007). Likewise, MMP-2 is also reported to be elevated *in vitro* in optic nerve head glial cells as well as in primary human lamina cribosa cells undergoing mechanical stretching (Akhter, Nix, Abdul, Singh, & Husain, 2013; Kirwan, Crean, Fenerty, Clark, & O'Brien, 2004). However, in injury models such as ischemia-reperfusion and excitotoxic injury, the role of MMP-2 is debatable. Some studies have reported that MMP-2 activity/expression was unchanged after ischemia-reperfusion (Zhang & Chintala, 2004) and excitotoxicty (Manabe, Gu, & Lipton, 2005) while others have reported increased MMP-2 activity within the post few hours of such injury (Zhang et al., 2002). Overall, these studies suggest the potential role of MMP-2 in glaucomatous pathology.

1.3.3 MMP-9

By far, MMP-9 is the best studied MMP in glaucomatous studies. Its role in both anterior and posterior segments of the eye is described in the next section.

1.4 MMP-9 in glaucomatous pathology: anterior segment

In the anterior chamber, the trabecular ECM primarily regulates the aqueous outflow facility. The trabecular meshwork cells constitutively secrete endogenous MMPs such as MMP-1, -2, -3, -9, -12 and MMP-14, as well as their endogenous inhibitor TIMP-2 (De Groef, Van Hove, Dekeyster, Stalmans, & Moons, 2013). Abnormal ECM deposits have also been found in the trabecular meshwork region in glaucomatous cases (Tektas & Lutjen-Drecoll, 2009). Indeed, perfusion of human anterior segments with purified

MMPs, containing equal concentrations of activated MMP-2, -3 and MMP-9 resulted in increased outflow facility lasting for at least 5 days and that was reversible (J. M. Bradley et al., 1998). Interestingly, inhibition of endogenous trabecular metalloproteinase activity using TIMP-2, minocycline, or L-tryptophan hydroxamate reduced outflow rates in human anterior segments (J. M. Bradley et al., 1998; J. M. B. Bradley et al., 2001).

Of note, laser treatment procedure to treat glaucomatous IOP elevations causes remodeling of extracellular matrix in the juxtacanalicular region of the trabecular meshwork (De Groef et al., 2013). Interestingly, the efficacy of laser treatment for glaucoma seems to be related primarily to the sustained induction of stromelysin and MMP-9, specifically within the outflow facility (Alexander, Samples, Van Buskirk, & Acott, 1991; Parshley et al., 1996). In addition, a study by Chintala and colleagues reported that the results of glaucoma filtering surgery were compromised in human patients due to the formation of leakage in blebs and this leakage was mostly attributed to the presence of 92-kDa gelatinase MMP-9 in the bleb tissue (Chintala et al., 2005). Thus, the role of MMP-9 has been implicated in the anterior chamber, specifically within the region of the trabecular meshwork controlling aqueous outflow.

In order to fully understand the exact involvement of MMP-9 *in vivo*, our lab has previously used MMP-9 knockout mouse (MMP-9KO) and measured IOP non-invasively. Our previous data demonstrates that MMP-9 deficiency leads to elevated IOP in mice, in the absence of any distinct morphological changes in the anterior chamber (Robertson, Siwakoti, & West-Mays, 2013). MMP-9 deficiency has also been shown to cause increased IOP in another study (Haddadin, 2013). Taken together, these data

strongly suggest that MMPs, more specifically MMP-9, plays a significant role in IOP homeostasis.

1.5 MMP-9 in glaucomatous pathology: posterior segment

The role of MMPs in the retina has also been well documented in glaucomatous pathology. By far, MMP-9 is the most well studied MMP in the retina (De Groef et al., 2014). At basal level, MMP-9 is undetectable in the ganglion cell layer (GCL) of the retina (Agapova, Kaufman, Lucarelli, Gabelt, & Hernandez, 2003). However, in response to optic nerve injury, its level is upregulated in the GCL layer of the retina and this hints to a role of MMP-9 in the pathophysiology of glaucoma (Chintala, Zhang, Austin, & Fini, 2002; Sun et al., 2011).

Studies have elucidated positive correlation between MMP-9 and RGC death in ocular hypertension (Guo et al., 2005), NMDA- and KA-mediated excitotoxicity (Ganesh & Chintala, 2011; Zhang, Cheng, & Chintala, 2004a), optic nerve ligation (Chintala et al., 2002) and optic nerve transection (Sun et al., 2011) models of glaucoma. In a rat model of ocular hypertension, there was a significantly strong correlation between MMP-9 activity and both RGC apoptosis and loss of laminin (Guo et al., 2005). Furthermore, intravitreal injection of NMDA upregulated the proform of MMP-9 in the retina and increased MMP-9 gelatinolytic activity in the ganglion cell layer (Manabe et al., 2005). This increase in MMP-9 activity further led to RGC apoptosis, while MMP inhibition using GM6001 prevented pathological remodeling of the ILM and detachment-induced apoptosis ("anoikis") of the RGCs, further supporting the role of MMP-9 in RGC death (Manabe et al., 2005). Similarly, in response to optic nerve ligation, MMP-9 activity increased in the GCL and this increase corroborated with the loss of laminin from the

inner limiting membrane of the retina (Chintala et al., 2002). In contrast, mice deficient in MMP-9 undergoing optic nerve ligation displayed little reduction in ganglion cells and laminin immunoreactivity was relatively unaffected, highlighting the neuroprotective property of MMP-9 deficiency in the retina (Chintala et al., 2002). Likewise, optic nerve transection led to a significant upregulation of MMP-9 and RGC death while down regulation of MMP-9 prevented RGC death after optic nerve transection (Sun et al., 2011).

Overall, it has been suggested that in response to optic nerve injury, astrocytes become reactive, synthesize elevated levels of MMP-9 and promote RGC death by degrading extracellular matrix present in the nerve fiber layer (Zhang, Cheng, & Chintala, 2004b). Although MMP-9 itself may not directly cause ganglion cell death, MMP-9 degrades ECM proteins such as laminin that is abundantly present in nerve fiber layer and predisposes RGCs to excitotoxicity, thereby triggering RGC apoptosis (Chintala et al., 2002; Zhang et al., 2004b). Additional evidence suggests that decrease in MMP-9 level through inhibition of reactive gliosis prevented apoptotic death of RGCs providing neuroprotection (Ganesh & Chintala, 2011). Collectively, these findings indicate that MMP-9 is a crucial modulator of retinal ganglion cell survival and its role warrants further studies in glaucomatous pathology.

CHAPTER TWO

MAIN HYPOTHESIS, SPECIFIC AIMS AND RATIONALE

2.1 Main Hypothesis

As outlined in the introduction, MMP-9 plays a role in aqueous humor outflow as well as retinal ganglion cell survival. The starting point of this thesis was the observation that MMP-9 deficient (MMP-9KO) mice exhibit increased IOP in the absence of overt morphological changes between 1-4 months of age (Robertson et al., 2013). In this thesis, **my overall objective is to examine whether the elevated IOP in MMP-9KO mice is sustained at a later time point and if the elevated IOP impacts retinal ganglion cell (RGC) number and retinal extracellular matrix (ECM) remodeling**. **Overall, I hypothesize that the elevated IOP in MMP-9KO mice will reduce RGC number and induce retinal ECM remodeling.**

2.2 Specific Aims and Rationale

2.2.1 Aim 1: To determine whether MMP-9KO mice continue to exhibit elevated IOP.

In previous work from the West-Mays' lab, it was shown that MMP-9KO mice exhibit increased IOP in the absence of distinct morphological changes between 1-4 months of age (Robertson et al., 2013). To determine if the elevated IOP is maintained at a later time, I will perform IOP readings at a later time point of 6-8 and 9-12 months of age between MMP-9KO and age matched control mice.

At different ages (2-3 months, 3-4 months, 6-8 months and 9-12 months of age), IOP will be measured *in vivo* using Tonolab Rebound Tonometer. The TonoLab operates on the rebound principle in which a probe with a smooth Teflon tip, strikes the cornea. Motion parameters during the collision (deceleration, impact time) are measured electronically and related to IOP via an internal algorithm. There are many factors that

can affect IOP and corneal thickness is one of them. Therefore, corneal thickness will be measured using ultrasound pachymeter. The measurement of corneal thickness between these animal groups *in vivo* will help to determine if the IOP readings obtained from my experiments are confounded due to changes in corneal thickness.

2.2.2 Aim 2: To determine if the elevated IOP in MMP-9KO mice results in a decrease in the Brn3a+ RGC count.

Previous studies have shown that elevated IOP can cause loss of RGCs due to mechanical stress at the optic nerve head, reduction in retinal blood perfusion and other factors (Guo et al., 2005; Ji et al., 2005; Resta et al., 2007). In my thesis, I will examine if the elevated IOP associated with MMP-9KO mice affects RGC number. At different ages (2-3 months, 3-4 months, 6-8 months and 9-12 months of age), retinas will be harvested and stained with Brn3a+ marker, a transcription factor for retinal ganglion cells. Then, the retinas will be flatmounted on slides and Brn3a+ cell bodies will be quantified.

2.2.3 Aim 3: To determine if the elevated IOP in MMP-9KO mice causes ECM remodeling and induces glial response.

Following the measurement of corneal thickness, mice will be sacrificed and eyes will be harvested for histology and immunofluorescence studies. 4 µm-thin paraffin cross-sections of eyes will be cut and stained with H&E to test if the elevated IOP in MMMP-9KO group leads to changes in retinal morphology. Additionally, sections will be incubated with laminin antibody to examine the effect of MMP-9 deficiency on the expression of laminin, which is an important extracellular matrix protein found in the inner limiting membrane of the retina. I will also stain retinal sections with markers of

gliosis such as GFAP and Iba1 to determine if the elevated intraocular pressure in MMP-9KO mice causes changes in glial response.

2.2.4 Aim 4: To determine the effect of optic nerve crush in both MMP-9KO and MMP-9WT groups at 2-3 months of age

A previous study has shown that MMP-9KO mice undergoing optic nerve ligation displayed little reduction in ganglion cell number and laminin immunoreactivity was relatively unaffected, highlighting the neuroprotective property of MMP-9 deficiency in the retina (Chintala et al., 2002). To further assess if MMP-9 deficiency is also neuroprotective in an optic nerve crush model, I will perform Brn3a+ labeling in retinal wholemounts of MMP-9KO and MMP-9WT groups of 2-3 months of age undergoing optic nerve crush. Then, I will perform a manual cell count of Brn3a+ cells using ImageJ and conduct statistical analysis.

CHAPTER THREE

EXPERIMENTAL DESIGN

3.1. Animals

All animal studies were performed according to the Canadian Council on Animal Care Guidelines and the ARVO Statement for the Use of Animals in Ophthalmic and Vision Research. MMP-9 KO mice and age-matched wild-type littermates (Jackson laboratories, Bar Harbor, ME) were on a C57BL/6 background. MMP-9KO mice were generated by the removal of part of exon 2 and all of intron 2 of the MMP-9 gene and these regions were replaced with a *pgk-neo* gene cassette (Vu et al., 1998). The breeding colonies of MMP-9WT and MMP-9KO mice groups were established in McMaster Central Animal Facility. Mice were housed under a 12-hour light/dark cycle and were fed normal mice chow and given access to drinking water *ad libitum*. A detailed experimental design is outlined in Figure 5.

3.2 Genotype Analysis

DNA extraction and purification from mouse ear tissue was performed with a kit (DNeasy, Qiagen Inc., Toronto, ON). Genotypes were determined by polymerase chain reaction (PCR) analysis. The MMP-9WT allele was detected by using primers (5'-GACTACTTGTACCGCTATGG-3' and 5'- TAACCGGAGGTGCAAACTGG-3') amplifying a 122-bp fragment. The MMP-9KO allele was detected by using primers (5'-GCATACTTGTACCGCTATGG-3' and 5'- GACCACCAAGCGAAACAT-3') to yield a 700 base pair fragment. PCR reactions were performed for 35 cycles in the following conditions: initial heating for 2 minutes at 94°C; denaturation for 30 seconds at 94°C; annealing for 30 seconds at 60°C; and extension for 2 minutes at 72°C. A final extension was performed for 10 minutes at 72°C. Agarose gel electrophoresis (1.5% agarose) with ethidium bromide detection was used to visualize the PCR reaction products.

3.3 IOP measurement

Mice at various age groups were anesthetized using 2.5% avertin solution at 0.015 ml/g body weight by intraperitoneal (i.p.) injection. To keep the cornea from drying out, eyes were lubricated with Tear-Gel ophthalmic liquid gel (Novartis Pharmaceuticals Canada Inc., Dorval, QC, Canada). A validated commercial rebound tonometer (TonoLab, Colonial Medical Supply, Franconia, NH) was used to take ten sets of six measurements of IOP in each eye. The average of a set of measurements was accepted only if the device indicated that there was "no significant variability" (per the protocol manual; Colonial Medical Supply). All measurements were taken between 3 and 5 minutes after i.p. injection, as prior studies have shown this to be a period with stable IOP (Ding, Wang, & Tian, 2011). As indicated by the manufacturer, the tonometer was horizontally aligned with the eye, and the tip of the probe was 2 to 3 mm from the eye. All readings were taken at daytime between 13:00 and 15:00 hours.

3.4 Corneal thickness

To assess whether central corneal thickness (CCT) contributes to any observed IOP difference, CCTs of MMP-9WT and MMP-9KO mice were measured by using ultrasound pachymeter (Corneao-Plus; Sonogage, Cleveland, Ohio) under anesthesia after IOP measurement. The probe was stabilized with a micromanipulator under the guidance of a dissecting microscope as previously described (Lively et al., 2010). The probe was perpendicularly aligned in front of the pupil and it was gently moved forward until the pachymeter began to record values. The number of eyes measured for each group at different ages is between 10 to15. After corneal thickness measurement, animals were euthanized by cervical dislocation, and their eyes were enucleated.

3.5 Optic nerve crush

Mice at 2-3 months age groups were anesthetized using 2.5% avertin (2,2,2-tribromoethanol in tert-amyl alcohol; Aldrich, Milwaukee, WI) solution at 0.015 ml/g body weight by intraperitoneal (i.p.) injection prior to surgery. Under the binocular operating scope, a small incision was made with spring scissors in the conjunctiva beginning inferior to the globe and around the eye temporally. The eye was rotated temporally to expose the posterior part of the eye. With micro-forceps, the edge of the conjunctiva next to the globe was grasped and retracted to allow the visualization of the optic nerve. The exposed optic nerve was grasped approximately 2 mm from the globe with Dumont SS fine forceps (cat. #RS-5027; Roboz) for 3 seconds, with the only pressure from the self-clamping action from the forceps to press on the nerve. At the end of the procedure, a small amount of surgical lubricant (Tear-Gel ophthalmic liquid gel; Novartis Pharmaceuticals Canada Inc., Dorval, QC, Canada) was applied to prevent corneal desiccation. To prevent dehydration, 1 mL of saline was administered subcutaneously before placing the animal on a warm heating pad until recovery. After 7 days post optic nerve crush, animals were sacrificed and eyes were extracted for retinal wholemount preparation.

3.6 Immunohistochemistry in retinal wholemounts

Retinas from both WT and KO mice at various age groups were dissected and permeabilized in PBS with 0.5% Triton X-100 (TPBS) by freezing for 15 minutes at -70°C. They were then rinsed in new TPBS and blocked overnight in 2% NDS in TPBS. The retinas were then incubated overnight at 4°C with goat anti-Brn3a (c-20) antibody (Santa Cruz Biotechnology, Heidelberg, Germany) diluted 1:500 in blocking buffer

(TPBS, 2% NDS). Then, retinas were washed six times for 5 minutes in PBS. Immunoreactivity was detected with Alexa Flour-568 donkey anti-goat IgG (H+L) antibody (Invitrogen-Molecular Probes, Barcelona, Spain) diluted 1:200 in blocking buffer. The secondary antibody was incubated for 4 h at room temperature. Finally, retinas were thoroughly washed six times for 10 minutes in PBS and mounted vitreal side up on subbed slides. All retinal wholemounts were mounted in Prolong Gold antifade reagent with 4',6-diaminodino-2-phenylindol (DAPI; Invitrogen, Eugene, OR) to visualize the nucleus.

3.7 Histology

Both WT and KO mice were sacrificed and their eyes were enucleated at different age groups in this study. After fixation of the enucleated eyes in 10% neutral buffered formalin for 48 hours, the eyes were embedded in paraffin by routine methods (sample size n=3 for each MMP-9WT and KO group and each time point). Four-micrometer-thick mid-sagittal sections were cut and stained with hematoxylin and eosin to visualize general retinal tissue architecture.

3.8 Immunohistochemistry on radial sections

Studies to fluorescently localize Iba1 and GFAP employed polyclonal antibodies to Iba1 (Wako, Richmond; 1:1000) and GFAP (Sigma, St. Louis, MO; 1:1000). Additionally, retinal sections were stained with polyclonal antibody to laminin (Sigma, St. Louis, MO; 1:60). Secondary antibodies included Alexa Flour-568 goat anti-rabbit rhodamine or donkey anti-mouse IgG (H+L) antibody (Invitrogen-Molecular Probes, Barcelona, Spain).

All immunohistochemistry was performed as follows: After dehydration in a graded series of xylene and ethanol, paraffin sections were washed three times for 5 min with PBS (Sigma Aldrich, St Louis, MO; pH 7.3), boiled for 20 min in 10 mM sodium citrate (pH 6.00) for antigen retrieval, and then washed an additional three times in PBS. Sections were then blocked with a solution of 5% normal donkey serum in PBS for 1 h at room temperature. After three washes of 5 min in PBS, the primary antibody was added to the sections in a volume of 100 µl and allowed to incubate overnight at 4 °C. After incubation, the sections were then washed three times for 5 min in PBS, and 100 µl of secondary antibody solution was added. The sections were incubated for 1 h at room temperature. After incubation, the sections were then washed three times for 5 min in PBS+0.1% Tween and then coverslipped with Vectashield mounting medium with 4', 6-diamidino-2-phenylindole (DAPI) as a nuclear counterstain (Vector Laboratories, Burlingame, CA).

3.9 Microscopy

Staining was visualized with a Leica DMRA2 fluorescence microscope (Leica Microsystems Canada, Inc., Richmond Hill, ON, Canada) equipped with a Q-Imaging RETIGA1300i FAST digital camera (Q-Imaging, Surrey, BC). Images were captured using OpenLab Software (PerkinElmer LAS, Shelton, CT) on retinal samples as illustrated in Figure 5. Cropping, rotating, and adding text to images were done using Adobe Photoshop 8 (Adobe Systems Canada, Ottawa, Canada).

3.10 Quantification and statistics

Number of $Brn3a^+$ cells in retinal wholemounts was quantified using image

quantification software (ImageJ, NIH) in areas shown in Figure 6. Each of the retinal ganglion cell was manually counted using the "Cell counter" feature on Image J. With this feature, each time an experimenter clicks on a Brn3a+ cell, the cell is marked, thus preventing the recounting of the same cell. All of the cells were automatically tallied using this feature. IOP and corneal thickness data were tested for significance by one-way ANOVA followed by Tukey post-hoc multiple comparison (Prism 5, GraphPad Software, La Jolla, CA, USA). All of the data on Brn3a+ cell count were tested for significance by two-way ANOVA. Significance was always considered at $p < 0.05$. All values are expressed as means and their 95% confidence intervals (CI) for direct indication of significance.

CHAPTER FOUR

RESULTS

4.1 Aim 1: To determine whether MMP-9KO mice continue to exhibit elevated IOP.

4.1.1 IOP is elevated in MMP-9KO mice compared to control littermates

Our lab has previously demonstrated that MMP-9 inhibition does not ameliorate the increased intraocular pressure associated with TGFβ1 overexpressing mice (Robertson et al., 2013). In fact, the IOP of MMP-9 knockout mice were significantly elevated compared to control littermates in the absence of morphological changes in the anterior chamber (Robertson et al., 2013).

In this thesis, additional IOP measurements were taken at 2-3, 3-4 months and IOP readings were taken at a later time point of 6-8 and 9-12 months of age. At 2-3 months, MMP-9KO mice (n=12) demonstrated significantly higher IOP than WT mice (n=12) (one-way ANOVA, $p<0.05$; Figure 7). At 3-4 months, the IOP was also elevated in the KO group (n=13) compared to WT (n= 13). At both 6-8 and 9-12 months, IOP remained significantly higher in the KO group compared to WT group. Of note, IOP was also significantly higher in the KO group at 9-12 months of age compared to KO group at 6-8 months of age, whereas no significant difference was observed in WT animals at similar time points (Figure 7). Mean IOP of MMP-9KO animals was significantly higher than that of control MMP-9WT animals at 2-3, 3-4, 6-8 and 9-12 months by 27%, 37%, 50% and 40% respectively ($p<0.05$; Table 1).

IOP readings acquired through contact tonometry may be affected by central corneal thickness (CCT). To investigate if the observed IOP difference between MMP-9KO and WT group was due to a difference in CCT, we employed the technique of ultrasound pachymeter to determine CCT in these groups. The average CCT values for MMP-WT mice were 108 ± 1.8 μm, 107 ± 3.7 μm, 109.5 ± 2.9 μm and 107.58 ± 2.9 μm

at 2-3, 3-4, 6-8 and 9-12 months respectively. Similarly, the average CCT values for MMP-9KO mice were 106 ± 4.7 μm, 106 ± 3.7 μm, 107 ± 1.8 μm and 105 ± 2.3 μm at 2-3, 3-4, 6-8 and 9-12 months respectively. At all time points investigated, there was no difference in corneal thickness between MMP-9KO and WT group using one-way ANOVA analysis ($p<0.05$; Figure 8). This suggests that the elevated IOP values observed in MMP-9KO mice were not affected by central corneal thickness.

4.2 Aim 2: To determine if the elevated IOP in MMP-9KO mice results in a decrease in the Brn3a+ RGC count.

4.2.2 Retinal ganglion cell counts do not differ between MMP-9WT and KO mice

The Brn3 family of POU-domain transcription factors plays essential roles in differentiation, neuronal identity, survival and axonal elongation during the development of murine RGCs (Wang et al., 2002). Brn3a has been shown to be specifically expressed by RGCs that project to the contralateral superior colliculus and dorsal lateral geniculate nucleus in adult mice (Quina et al., 2005). Brn3a has previously been used as a marker of RGCs in multiple studies (Galindo-Romero et al., 2011; Ganesh & Chintala, 2011; Nadal-Nicolas et al., 2009).

Fluorescence microscopy of wholemounted retinas of both MMP-9WT and KO mice showed immunolabeled RGCs in the ganglion cell layer distributed throughout the retina (Figure 9A). In agreement with previous reports of ganglion cell counts in C57BL/6 mice (Inoue, Sasaki, Hosokawa, & Fukuda, 2000; Williams, Strom, Rice, & Goldowitz, 1996), the distribution of Brn3a+ retinal ganglion cells in both WT and KO mice appears to be highest in the central retinal area and least in the peripheral retinal area. Interestingly, there appears to be no striking difference in Brn3a+ RGC number

between WT and KO groups in any of the retinal areas examined. To validate this observation, manual count of Brn3a+ cells between WT and KO groups was performed using ImageJ.

A detailed quantitative analysis of Brn3a+ RGC count is shown in Table 2. At all age groups examined, there was no significant difference in RGC count in central, mid-peripheral and peripheral retinal areas between MMP-9WT and KO groups further shown in Figure 9B (Two way ANOVA; $p<0.05$). Of particular interest, up until the furthest time point of 9-12 months, the average RGC count for KO group was 4577 ± 475 in central, 4076 ± 466 in mid-peripheral and 2814 ± 158 in peripheral retinal areas whereas for WT group, the values were 4293 ± 422 in central, 3909 ± 766 in mid-peripheral and 2843 ± 377 in peripheral retinas. These values demonstrate that at all of the time points/ages that I examined, the elevated IOP in MMP-9KO group did not lead to a loss of RGCs.

4.3 Aim 3: To determine if the elevated IOP in MMP-9KO mice causes retinal ECM remodeling and induces glial response.

4.3.1 Retinal morphology is not altered in MMP-9KO mice compared to control littermates

Elevated IOP in MMP-9KO group did not cause significant RGC death in time points investigated so far. Therefore, my aim was to further explore if this elevated IOP causes changes in retinal architecture. Histological analysis of retinas of both MMP-9WT and KO groups at different age groups revealed that at light microscopic level, both WT and KO mice demonstrate well-organized retina with cells neatly packed in different layers (Figure 10). All of the retinal layers namely ganglion cell layer, inner nuclear layer

and outer nuclear layer were aligned in parallel in both WT and KO groups at all time points examined. Also, there appeared to be no difference in retinal thickness between WT and KO groups at all age groups. Interestingly, the substrate of MMP-9 such as laminin is a crucial component of the inner limiting membrane (ILM) of the retina. Therefore, expression of laminin in the inner limiting membrane layer of the retina was further evaluated.

4.3.2 MMP-9KO group exhibits similar laminin expression as MMP-9WT group

The ILM consists of about ten high-molecular weight extracellular matrix (ECM) proteins that include members of the laminin family, nidogen1 and 2, collagen IV and three heparan sulphate proteoglycans, agrin, perlecan and collagen XVIII (Halfter, Dong, Dong, Eller, & Nischt, 2008). Functionally, the ILM is more appropriately considered as an adhesive sheet that facilitates the connection of the vitreous body (VB) with the retina. MMP-9 has previously been linked with laminin degradation (De Palma et al., 2008; Zhang et al., 2004a). To determine whether MMP-9KO mice display changes in laminin expression, paraffin sections of the eye were incubated with polyclonal laminin antibody.

At all age groups, laminin activity was predominantly observed in the ILM of the retina (Figure 11). There was no significant difference in laminin expression in both MMP-9WT and KO groups at all age groups examined.

4.3.3 Elevated IOP in MMP-9KO group does not cause significant glial response

Glial cells function to maintain retinal homeostasis and integrity. They respond to changes in homeostatic alterations such as pressure, infection, electrical activity, etc. To examine whether elevated IOP in MMP-9KO mice causes changes in glial response,

paraffin sections of the eye were incubated with glial fibrillary acidic protein (GFAP) and Iba1 antibody.

GFAP reactivity in central retina was seen mostly in ILM with a few reactive cells in outer and inner plexiform layers of the retina (Figure 12). In the retinas, the expression of GFAP was similar in both WT and KO groups (Figure 12). Additionally, there was no difference in GFAP expression at mid-peripheral and peripheral retinal areas in both WT and KO groups (data not shown). Up until 9-12 months of age, GFAP expression in optic nerve head area of MMP-9KO group was not significantly different compared to WT group (Figure 14C &14D).

Iba1 stands for ionized calcium binding adaptor molecule 1 (Bosco, Steele, & Vetter, 2011). Its level increases in connection with cytoskeletal remodeling and cell shape changes and this protein in extensively used as a marker of microglia activation in the CNS (Ito, Tanaka, Suzuki, Dembo, & Fukuuchi, 2001; Nilsson, Lindfors, Fetissov, Hokfelt, & Johansen, 2008). Iba1 localization was seen almost in all of the layers of the retina except the outer nuclear layer in both MMP-9WT and KO groups (Figure 13). In the central retina, the expression of Iba1 was similar in both WT and KO groups. Additionally, there was no difference in Iba1 expression at mid-peripheral and peripheral retinal areas in both WT and KO groups (data not shown). In the optic nerve head sections, Iba1-positive cells mainly localized throughout the inner optic nerve head (ONH) in both WT and KO eyes (Figure 14A & 14B; yellow arrowheads). In the lamina (OL), most microglia concentrated in a single thick plane at the ONH-OL border in a similar fashion in both WT and KO eyes (Figure 14A & 14B; between arrowheads). In

summary, there was no significant difference in Iba1 expression in both WT and KO groups in central retina as well as optic nerve head area.

4.4 Aim 4: To determine the effect of optic nerve crush in both MMP-9KO and MMP-9WT groups at 2-3 months of age

4.4.1 Brn3a+ cell count was not altered in the MMP-9KO mice compared to MMP-9WT mice undergoing optic nerve crush

A previous study has reported that MMP-9KO mice undergoing optic nerve ligation displayed little reduction in ganglion cells and laminin immunoreactivity was relatively unaffected, highlighting the neuroprotective property of MMP-9 deficiency in the retina (Chintala et al., 2002). To further assess if MMP-9 deficiency is also neuroprotective in optic nerve crush, I performed retinal ganglion cell count after 7 days of optic nerve crush in both MMP-9KO and MMP-9WT groups at 2-3 months of age.

Fluorescence microscopy of wholemounted retinas of both MMP-9WT and KO mice undergoing optic nerve crush showed immunolabeled RGCs in the ganglion cell layer (Figure 15A). The appearance of the RGCs in WT appeared reduced compared to naïve uninjured WT mice retinas as shown in Figure 9A. The average number of Brn3a+ RGCs in naïve MMP-WT mice at 2-3 months was 3532 ± 654 in central, 3325 ± 512 in mid-peripheral and 2419 ± 661 in peripheral retina. Interestingly, in MMP-9WT mice undergoing crush, the cell count values were 1307 ± 127 in central, 1141 ± 202 in mid-peripheral and 790 ± 227 in peripheral retina. These cell counts validate that the optic nerve crush resulted in a significant decline of RGCs in MMP-9WT mice undergoing crush (Two-way ANOVA; $p<0.05$). Surprisingly, there appears to be no striking difference in Brn3a+ RGC number between WT and KO groups undergoing crush in any

retinal area (Figure 15A). To validate this observation, manual count of Brn3a+ cells between WT and KO groups undergoing optic nerve crush was performed using ImageJ.

The average Brn3a+ RGC count for KO group undergoing crush was 1228 ± 296 in central, 1074 ± 215 in mid-peripheral and 864 ± 111 in peripheral retinal areas, which was similar to Brn3a+ RGC count in MMP-9WT group undergoing crush (as shown in Table 2). Upon statistical analysis, there was no significant difference in RGC count in central, mid-peripheral and peripheral retinal areas between MMP-9KO and MMP-9WT animals undergoing optic nerve crush (Two-way ANOVA; $p<0.05$). In summary, ON crush caused significant RGC decline in both WT and KO groups compared to naïve retinas but there was no significant difference in RGC counts between MMP-9WT and MMP-9KO groups after optic nerve crush.

CHAPTER FIVE

DISCUSSION AND CONCLUSION

The present study served to understand the role of MMP-9 in the regulation of IOP and retinal ganglion cell survival. Our lab had previously established that MMP-9KO mice exhibit increased IOP until 3-4 months of age in the absence of distinct morphological changes in the anterior chamber (Robertson et al., 2013). However, the role of MMP-9 deficiency on IOP regulation at a later age and the effect of elevated IOP on retinal ganglion cell survival remained unknown. My current work has demonstrated that in the absence of MMP-9, IOP level was elevated in the MMP-9KO mice compared to control littermates at all time points investigated. Surprisingly, the elevated IOP did not result in a significant loss of retinal ganglion cells in the MMP-9KO mice. Furthermore, the elevated IOP did not induce any significant change in laminin expression and glial reactivity, markers of retinal damage.

Although previous studies have elucidated the role of MMP-9 in *in vitro* culture of trabecular meshwork cells as well as in perfused anterior segments, the role of MMP-9 *in vivo* in IOP regulation remained to be determined (J. M. Bradley et al., 1998; Oh et al., 2006; Parshley et al., 1996). Our work using MMP-9KO mice and measurement of IOP *in vivo* provides compelling evidence that MMP-9 inhibition results in elevated IOP. The IOP readings in MMP-9KO mice increased from 27% at 2-3 months to 40% at 9-12 months compared to control groups at respective ages as shown in Table 1. To assess whether central corneal thickness (CCT) contributed to any observed IOP difference, CCTs of MMP-9WT and MMP-9KO mice were measured by using ultrasound pachymeter. We found no difference in CCT vales of both MMP-9WT and MMP-9KO groups as shown in Figure 8, indicating that the elevated IOP in the MMP-9KO mice cannot be attributed to change in corneal thickness. Although the cause of IOP elevation

remains unknown, there are a number of possibilities based on what we know about the role of MMP-9. The spaces between the collagen beams in the TM are filled with extracellular matrix (ECM) and it has previously been shown that perfusion of human anterior segments with purified MMP-9 from cultured medium resulted in increased outflow facility (J. M. Bradley et al., 1998). This provides evidence that MMP-9 may be important in maintaining aqueous outflow facility, perhaps by regulating ECM turnover in the TM region. Thus, in the absence of MMP-9, there may be an accumulation of ECM proteins such as collagen IV, elastin and fibronectin resulting in a reduced filtration capacity of aqueous humor, resulting in elevated IOP (Schlotzer-Schrehardt, 2002). However, changes in the deposition of ECM proteins in the TM region at a light microscopic level were not observed in the MMP-9KO mice (Robertson et al., 2013). We cannot rule out, however, that ultrastructural changes have occurred and this should be examined in the future. It is also possible that the lack of MMP-9 caused alteration in the actin cytoskeleton of the TM affecting its contractility, resulting in an increase in TM tissue stiffness that would affect aqueous humor outflow. Furthermore, MMP-9 has also been shown to be important in regulating cell-cell junctions (Vermeer et al., 2009). Thus, the loss of MMP-9 function could potentially influence cell-to-cell contact in the inner endothelial wall of Schlemm's canal, delaying aqueous outflow and increasing IOP. In the future, techniques such as ultrastructural analysis and/or measurement of aqueous outflow facility will provide further avenues for investigating TM architecture in MMP-9KO mice, and hopefully will aid in our understanding of the role of MMP-9 in maintaining IOP homeostasis.

To examine if the elevated IOP in MMP-9KO mice leads to RGC death, I stained

retinal flatmounts with Brn3a antibody and performed Brn3a+ cell count. Brn3a has been shown to be specifically expressed by RGCs that project to the contralateral superior colliculus and dorsal lateral geniculate nucleus in adult mice (Quina et al., 2005) and it has previously been used as a marker of RGCs in multiple studies (Galindo-Romero et al., 2011; Ganesh & Chintala, 2011; Nadal-Nicolas et al., 2009). In the retina, previous studies have shown that an increase in MMP-9 activity leads to RGC apoptosis, while MMP inhibition using GM6001 has been shown to prevent pathological remodeling of the ILM and detachment-induced apoptosis ("anoikis") of the RGCs (Manabe et al., 2005). In this thesis, it was shown that in the absence of MMP-9, mice with elevated IOP did not exhibit an increase in RGC death compared to control littermates. There are a number of possible explanations for the lack of RGC death. Firstly, the IOP elevation in MMP-9KO mice may not have been significant enough to cause pressure-induced RGC death at the time points examined. In a previous study, Tsuruga *et al* achieved pressure-dependent RGC damage by using laser-induced ocular hypertension (Tsuruga, Murata, Araie, & Aihara, 2012). The IOP difference in the ocular hypertensive mice was approximately 17 mm Hg more than control mice and this increase was required to cause significant RGC death (Tsuruga et al., 2012). In our mouse model, the highest average pressure difference in MMP-9KO group versus WT group was approximately 6 mm Hg and perhaps this pressure difference was not significant enough to cause pressure-dependent RGC death. On the contrary, a study has shown that in a transgenic mouse model with Type I collagen mutation, an IOP increase of approximately 5 mm Hg was sufficient to cause 29% of axonal loss (Mabuchi, Lindsey, Aihara, Mackey, & Weinreb, 2004). In the future, optic nerve sections stained with paraphenylenediamine (PPD) can

be performed to examine if the elevated IOP in MMP-9KO mice leads to optic nerve axonal loss.

It is also possible that the effect of elevated IOP on RGC death in the MMP-9KO mice may occur at a later age than 12 months, my last time point examined. As shown in Figure 7, IOP continues to rise at a later age compared to earlier time points in MMP-9KO mice. The IOP was significantly higher in the KO group at 9-12 months of age compared to KO group at 6-8 months of age, whereas such a significant rise in IOP was absent in WT mice at similar time points. Therefore, it is possible that at a later time point, the IOP in MMP-9KO mice will continue to rise and this might eventually result in a significant RGC death compared to control littermates.

MMP-9KO mice may also be resistant to pressure-induced RGC death. For example, it has previously been shown that unlike control littermates, MMP-9KO mice undergoing optic nerve ligation exhibited very little RGC death and this was attributed to a lack of degradation of laminin from the ILM, which prevented "anoikis" (detachment-induced apoptosis) of RGCs (Chintala et al., 2002). Indeed, when I examined laminin reactivity in the ILM of both MMP-9WT and MMP-9KO mice, I found that laminin reactivity was similar, thus demonstrating that the retinas of MMP-9KO were not undergoing damage in the ILM. Additionally, changes in retinal morphology and gliosis in the MMP-9KO mice were investigated. A previous study has shown that acute experimental elevation of IOP can cause changes in retinal morphology such as retinal thinning and gliosis (Kim, Braun, Wordinger, & Clark, 2013). Despite elevated IOP, I did not find changes in retinal morphology and GFAP and Iba1 reactivity in MMP-9KO mice compared to their control age-matched littermates. Glial cells respond quickly to even the

slightest homeostatic alterations such as IOP (Tezel, 2011). Thus, the lack of GFAP and Iba1 expression in the retina and optic nerve of the MMP-9KO mice, despite elevated IOP, was somewhat surprising. It is possible that in mouse models of acute experimental IOP elevation, IOP changes within a short period of time causes drastic changes in retinal morphology and gliosis. However, our MMP-9KO mice exhibit chronic IOP elevation. Therefore, due to a lack of immediate rise in IOP in MMP-9KO mice, there might be a subsequent lack in processes such as retinal thinning and gliosis as observed in acute mouse models of IOP elevation. Another possibility, however, is that the lack of MMP-9 expression in the MMP-9KO retina offers a neuroprotective effect.

To further investigate whether MMP-9KO mice retinas were neuroprotected against injury, I performed optic nerve crush experiments. I hypothesized that if the MMP-9KO mice were neuroprotected, damage resulting from optic nerve crush may be prevented. However, in contrast to the optic nerve ligation study performed by Chintala, my results demonstrated no difference in Brn3a+ RGC count between MMP-9KO and control mice undergoing optic nerve crush. It is possible that the optic nerve crush model that we employed was too severe, as compared to optic nerve ligation, to observe the neuroprotective property of MMP-9 deficiency in the retina. Therefore, future experiments with milder form of injury such as intravitreal injection of NMDA on both WT and KO mice could be conducted to examine if the RGCs in MMP-9KO mice are resistant to excitotoxicity. Such experiments could potentially reveal the neuroprotective effect of MMP-9 deficiency in the retina.

Overall, the findings from this thesis have demonstrated that MMP-9KO mice exhibit elevated IOP at all time points investigated. Although the reason for ocular

hypertension is unknown at this point, in the future, techniques such as ultrastructural analysis or measurement of aqueous outflow facility will provide a further evidence regarding the TM architecture and function in MMP-9KO mice, which will aid in our understanding of the role of MMP-9 in maintaining IOP homeostasis. With regards to retinal damage, it is possible that MMP-9KO retinas may be neuroprotected and this should be further studied. It is also possible that elevated IOP in MMP-9KO mice might lead to optic nerve axon loss and this should be further explored. Despite the extensive use of Brn3a as a marker of RGC, as carried out in this thesis, there is some conflicting evidence on the reliability of Brn3a as a good marker of RGC. For example, a study has shown that Brn3a labeling is observed in only about 40 to 55% of RGCs (Levesque, 2013). However, Galindo-Romero *et al* found that Brn3a labeling was visible in about 86% of retrogradely labeled hydroxystilbamidine methanesulfonate (OHSt)-positive RGCs making it a reliable cell marker. It is, however, unclear whether elevated IOP itself could influence the expression of the Brn3a transcription factor in the RGCs. Amidst such contrasting evidence, further analysis of optic nerve axons using PPD-stained sections might be a better alternative to examine the effect of elevated IOP on the optic nerve axons in the MMP-9KO mouse model. Overall, based on my current findings, the MMP-9KO mouse may serve as a suitable model to study ocular hypertension and, if axonal loss is discovered, it could potentially be utilized as a mouse model to study open angle glaucoma.

FIGURES & TABLES

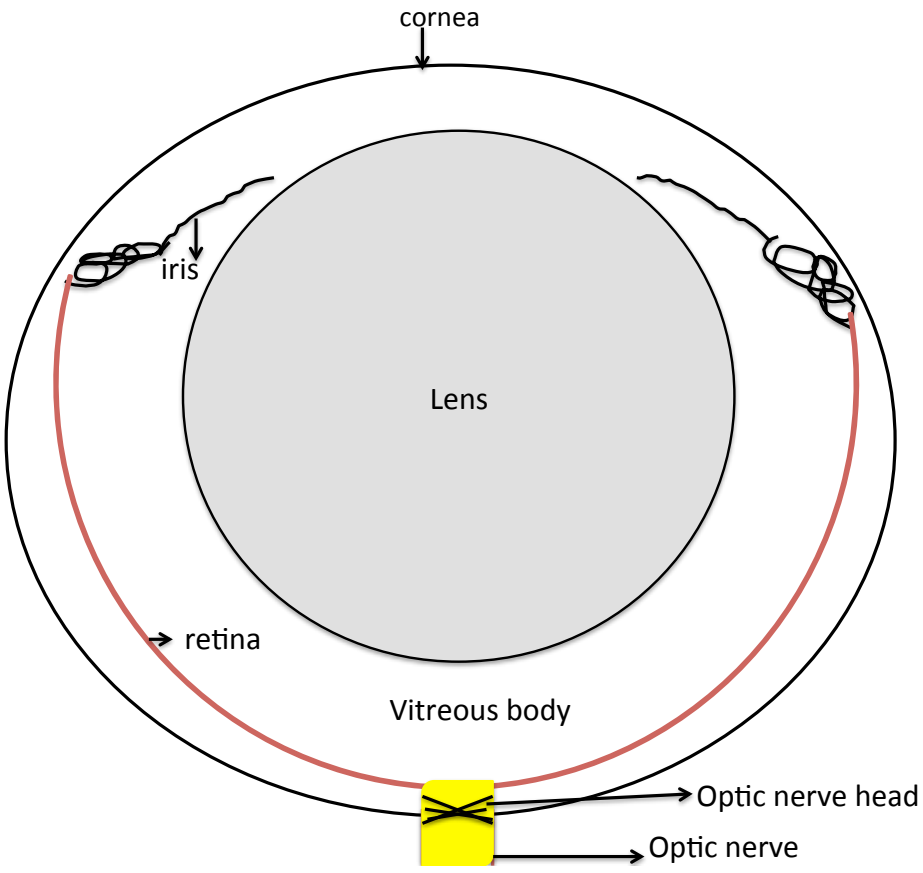

Figure 1: General anatomy of a mouse eye. The anterior segment in the eye comprises of cornea, iris, and lens whereas the posterior segment comprises of vitreous, retina and the optic nerve.

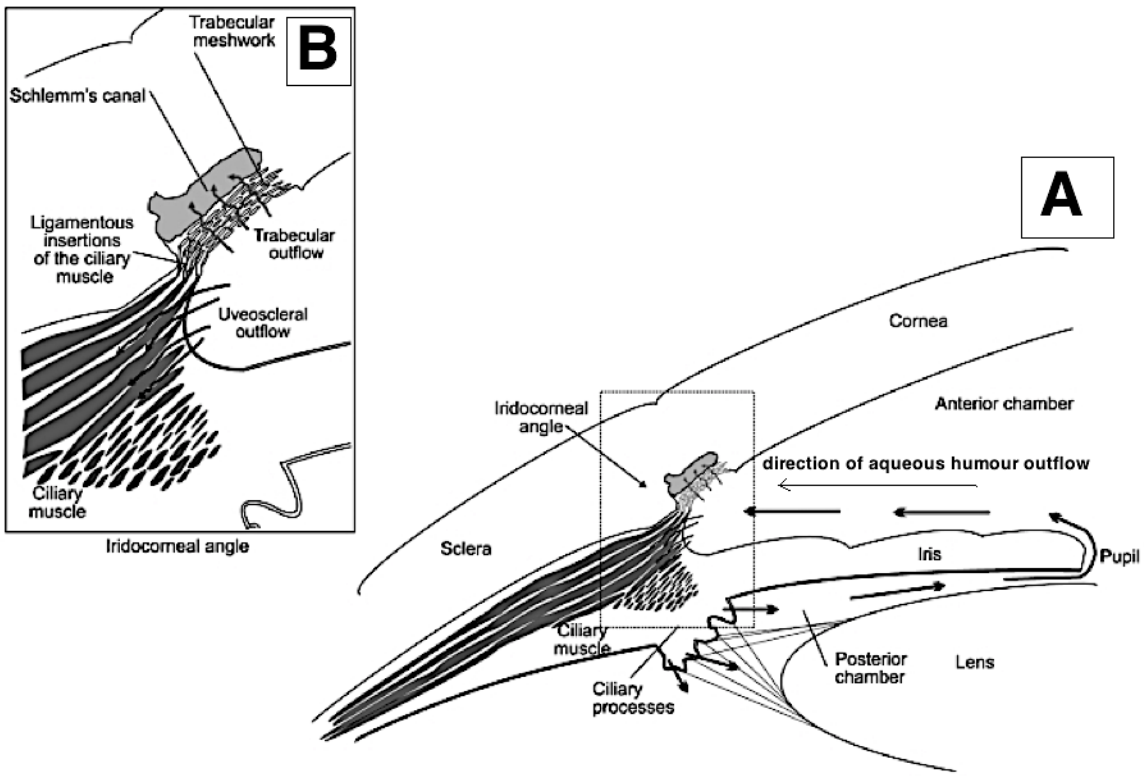

Figure 2: Aqueous outflow pathways. A) Transverse view of the anterior section of the eye. The black arrow shows the movement of aqueous humor from ciliary epithelium to the anterior chamber and out through the outflow pathways. B) A close depiction of trabecular and uveoscleral outflow pathway. Aqueous humor exits from anterior chamber through the trabecular meshwork to Schlemm's canal (trabecular outflow) or through the spaces between ciliary muscle bundles (uveoscleral outflow). Figure adapted from Llobet et al., 2003.

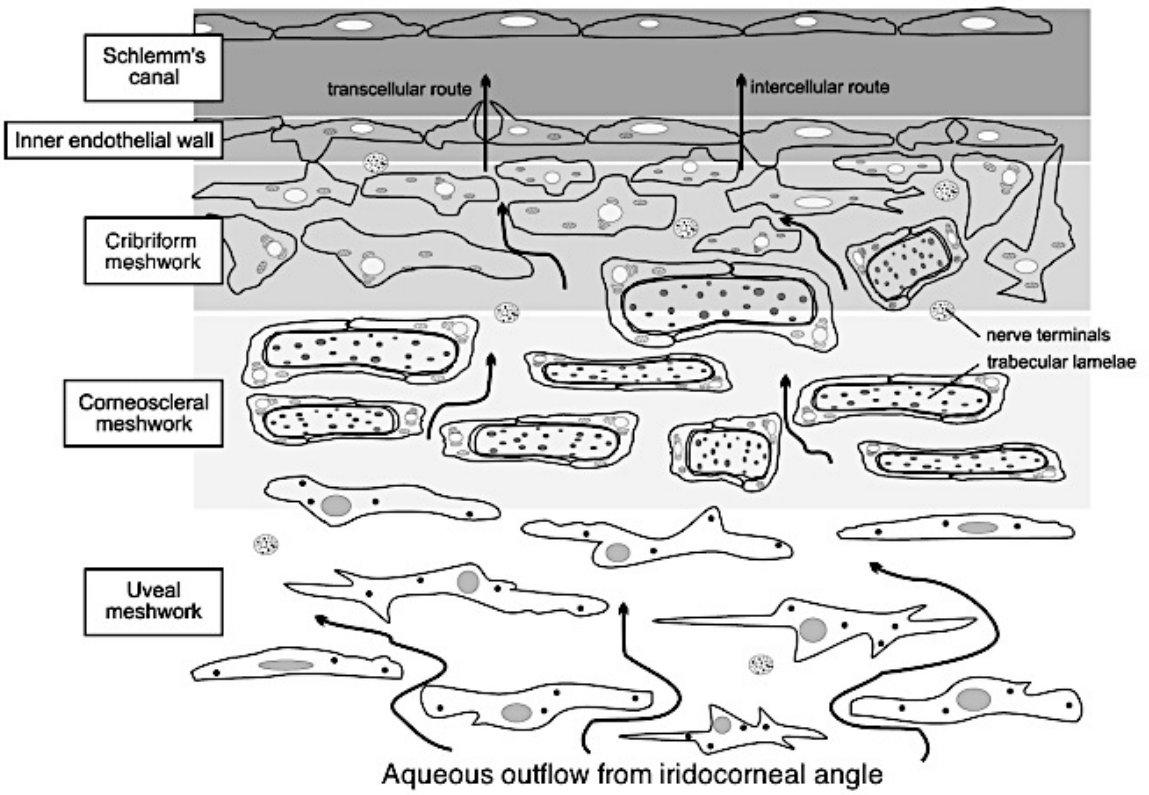

Figure 3: Schematic diagram of the trabecular outflow. Aqueous humor exits the eye from the anterior chamber through intercellular spaces as indicated by the direction of arrows. Different layers of the trabecular meshwork are the uveal meshwork, corneoscleral meshwork, cribriform or juxtacanalicular meshwork, inner endothelial wall and Schlemm's canal. As the intercellular spacing between cells decreases from uveal meshwork to inner wall of Schlemm's canal, resistance to aqueous humor outflow increases. Figure adapted from Llobet et al., 2003.

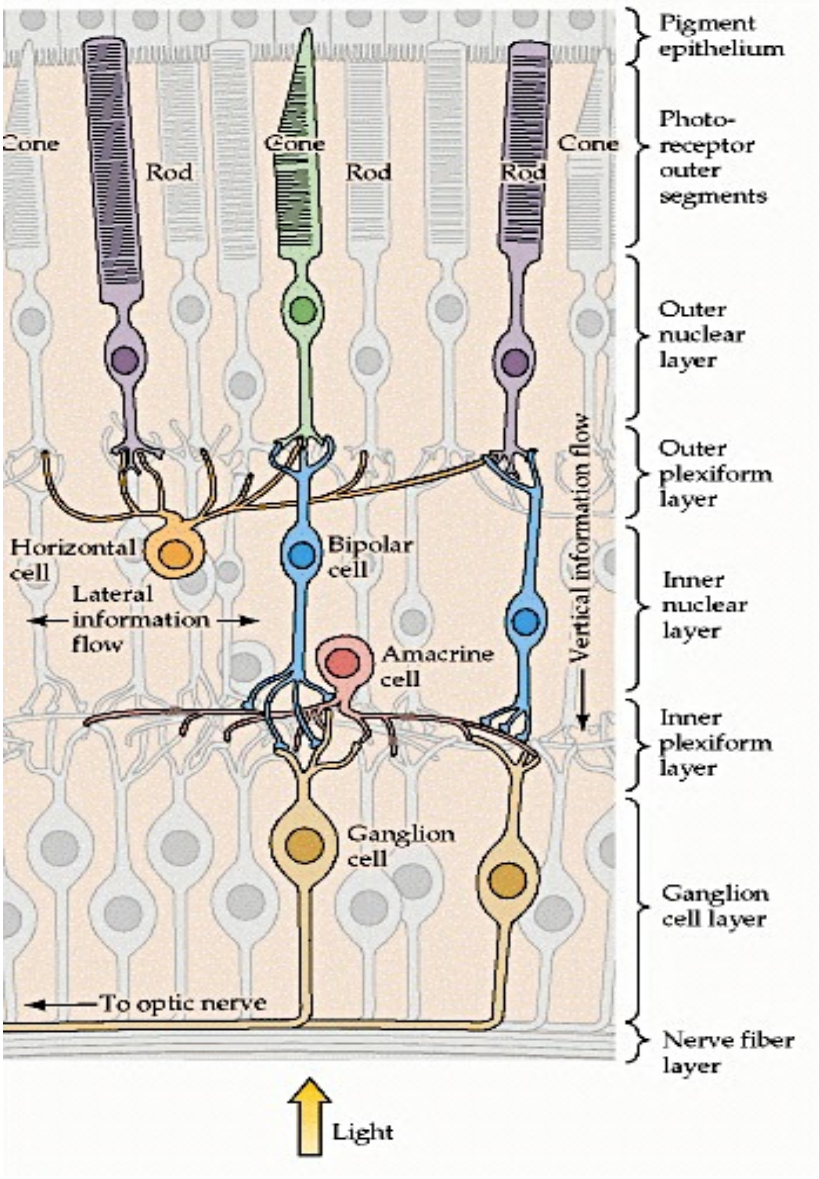

Figure 4: Organization of the retina. The neural layer of the retina consists of various layers; from outer to inner they are: retinal pigment epithelium, photoreceptors, outer limiting membrane, outer nuclear layer, outer plexiform layer, inner nuclear layer, inner plexiform layer, ganglion cell layer, nerve fiber layer and inner limiting membrane. A light ray passes from the inner limiting membrane to the rods and cones and the signal is carried back vice-versa *via* the optic nerve and the signal is integrated and interpreted at the visual cortex in the brain. Source: Figure from Neuroscience, 5th edition, Purves et al. with approval from Sinauer Associate, Inc. Please refer to Appendix.

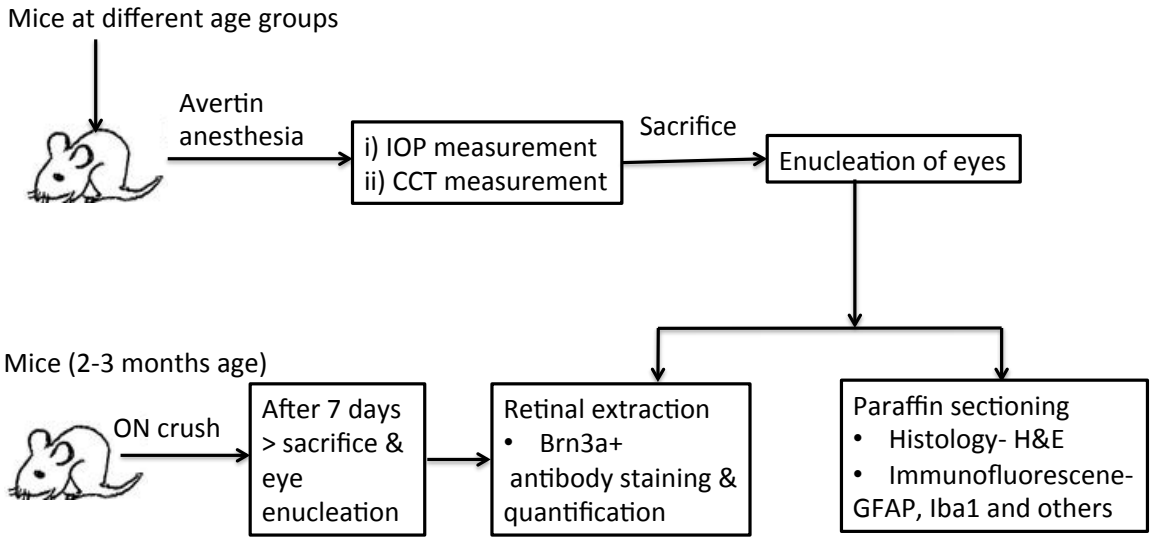

Figure 5: Experimental timeline for the proposed study. At different age groups, mice were anesthetized using avertin (0.015 ml/g). Then, IOP and corneal thickness were measured. The animals were then sacrificed by cervical dislocation. Eyes were enucleated and they were used for paraffin sectioning for histology and immunofluorescence studies. An additional number of eyes were used for Brn3a+ RGC specific staining on retinal wholemounts. Abbreviations: IOP: Intraocular pressure, CCT: Central Corneal thickness.

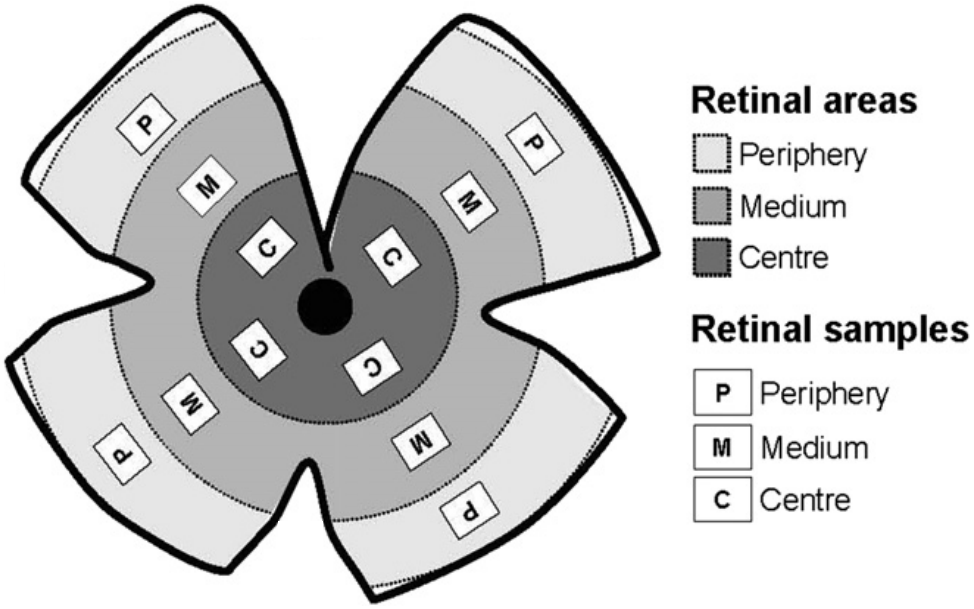

Figure 6: Schematic drawing of retinal wholemount. Schematic depicting the retinal areas and retinal samples used to quantify Brn3a^{+} staining. Figure adapted from Galindo-Romero et al., 2011.

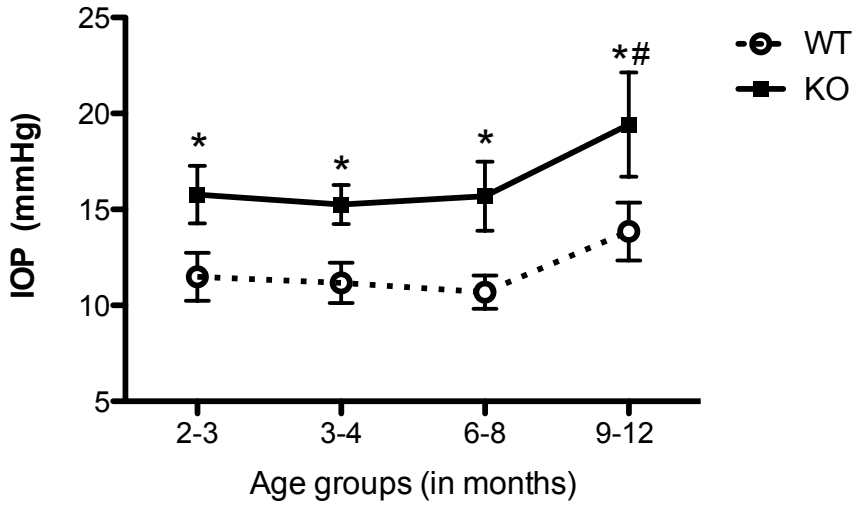

Figure 7: IOP measurement at different age groups. At all time points, MMP-9KO animals demonstrated a higher IOP than their wild type littermates. Of note, IOP was also significantly higher in the KO group at 9-12 months of age compared to KO group at 6-8 months of age, whereas no significant difference was observed in WT animals at similar time points. * $p<0.05$ KO compared to WT, # $p<0.05$ MMP-9KO (9-12) compared to MMP-9KO (6-8). Bars represent mean ± 95% CI. One-way ANOVA was used for statistical analysis.

	Age (in months)			
	2-3	**3-4**	**6-8**	**9-12**
Number of MMP-9KO eyes	12	13	18	8
IOP of MMP-9KO eyes [IOPt] (mm Hg; mean ± 95% CI)	15.8 ± 1.3	15.3 ±0.9	16.1 ± 1.8	19.4 ± 2.3
Number of MMP-9WT	13	14	18	8
IOP of MMP-9WT eyes [IOPc] (mm Hg; mean ± 95% CI)	11.5 ± 1.1	11.2 ± 0.9	11.3 ± 0.6	13.9 ± 1.3
Δ IOP (mm Hg) [IOPt-IOPc]	4.3	4.1	5.7	5.5
Δ IOP% [100 x Δ IOP/IOPc]	27	37	50	40

Table 1: IOP in MMP-9WT and MMP-9KO mice groups of different ages. IOP in MMP-9KO group is significantly higher compared to WT control at each age group. One-way ANOVA was used for statistical analysis ($p<0.05$).

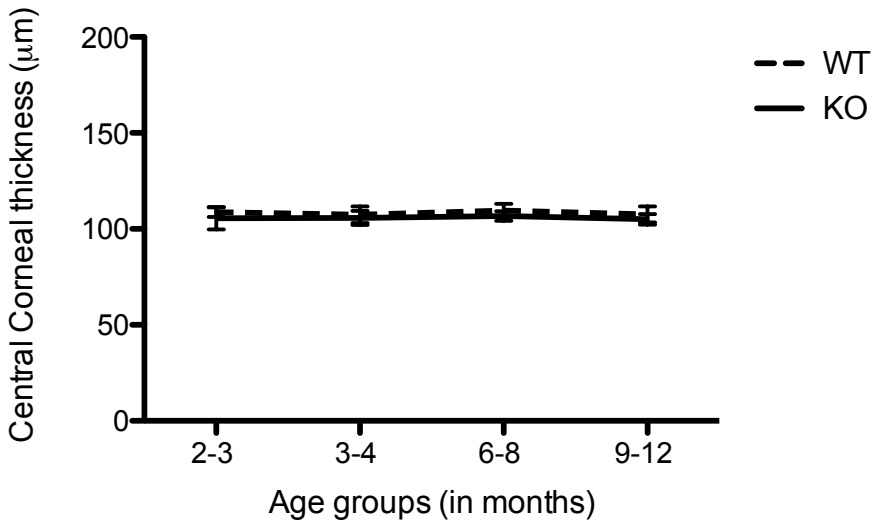

Figure 8: Central corneal thickness measurement at various age groups. At all of the time points, there is no difference in corneal thickness between the MMP-9WT and KO mice. This suggests that the elevated IOP observed in MMP-9KO mice was not due to changes in corneal thickness. Bars represent mean ± 95% CI. One-way ANOVA was used for statistical analysis ($p<0.05$).

A.

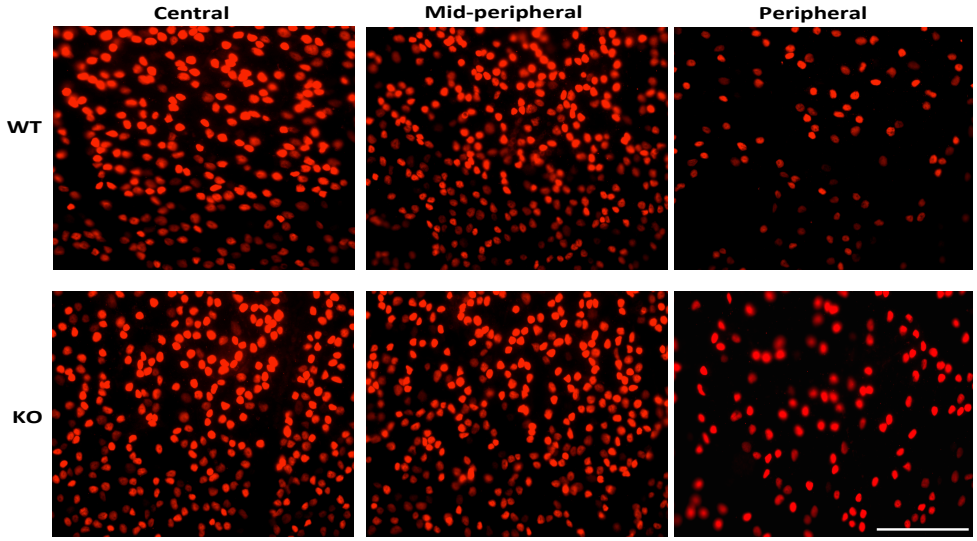

B.

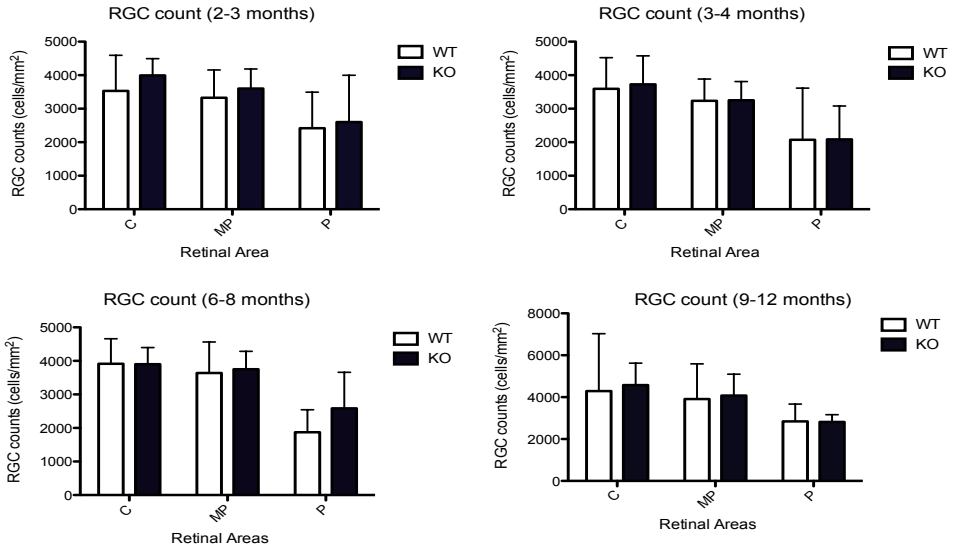

Figure 9: Brn3a+ cell count on retinal wholemounts. (A) Immunofluorescence pictures from central, mid peripheral and peripheral retinal samples of both WT and KO mice. ImageJ was used to quantify the cell number between these groups. (B) Quantification of Brn3a+ RGCs on different retinal areas at different age groups between WT and KO eyes. Bars represent mean ± 95% CI. One-way ANOVA was used for statistical analysis. Abbreviations: C= central retinal area, MP= mid-peripheral retinal area, P= peripheral retinal area, WT= MMP-9 wild type mice and KO= MMP-9 knock out mice. Scale= 100 µm.

Groups & age (in months)	Average RGC count in various areas (cells/mm^2) ± 95% CI		
	Central	**Mid-peripheral**	**Peripheral**
WT (2-3)	3532 ± 654	3325 ± 512	2419 ± 661
KO (2-3)	3992 ± 310	3602 ± 358	2604 ± 858
WT (3-4)	3592 ± 573	3235 ± 400	2074 ± 949
KO (3-4)	3727 ± 524	3251 ± 344	2087 ± 612
WT (6-8)	3913 ± 460	3638 ± 572	1873 ± 414
KO (6-8)	3901 ± 306	3752 ± 327	2585 ± 662
WT (9-12)	4293 ± 422	3909 ± 766	2843 ± 377
KO (9-12)	4577 ± 475	4076 ± 466	2814 ± 158
WT (2-3; ONC)	1307 ± 127	1141 ± 202	790 ± 257
KO (2-3; ONC)	1228 ± 335	1073 ± 244	864 ± 125

Table 2: Brn3a+ RGC count in MMP-9WT and MMP-9KO mice groups of different ages. Brn3a+ RGC count in MMP-9KO group is not significantly different compared to WT control at each age group. However, upon optic nerve crush, Brn3a+ RGC count reduced significantly in both MMP-9WT and MMP-9KO mice compared to naïve mice at similar age groups. RGC count, however, was not significantly different between MMP-9WT and MMP-9KO group upon optic nerve crush. Two-way ANOVA was used for statistical analysis followed by Tukey post-hoc comparison ($p<0.05$). Abbreviations: WT= MMP-9 wild type mice, KO= MMP-9 knock mice, ONC= optic nerve crush.

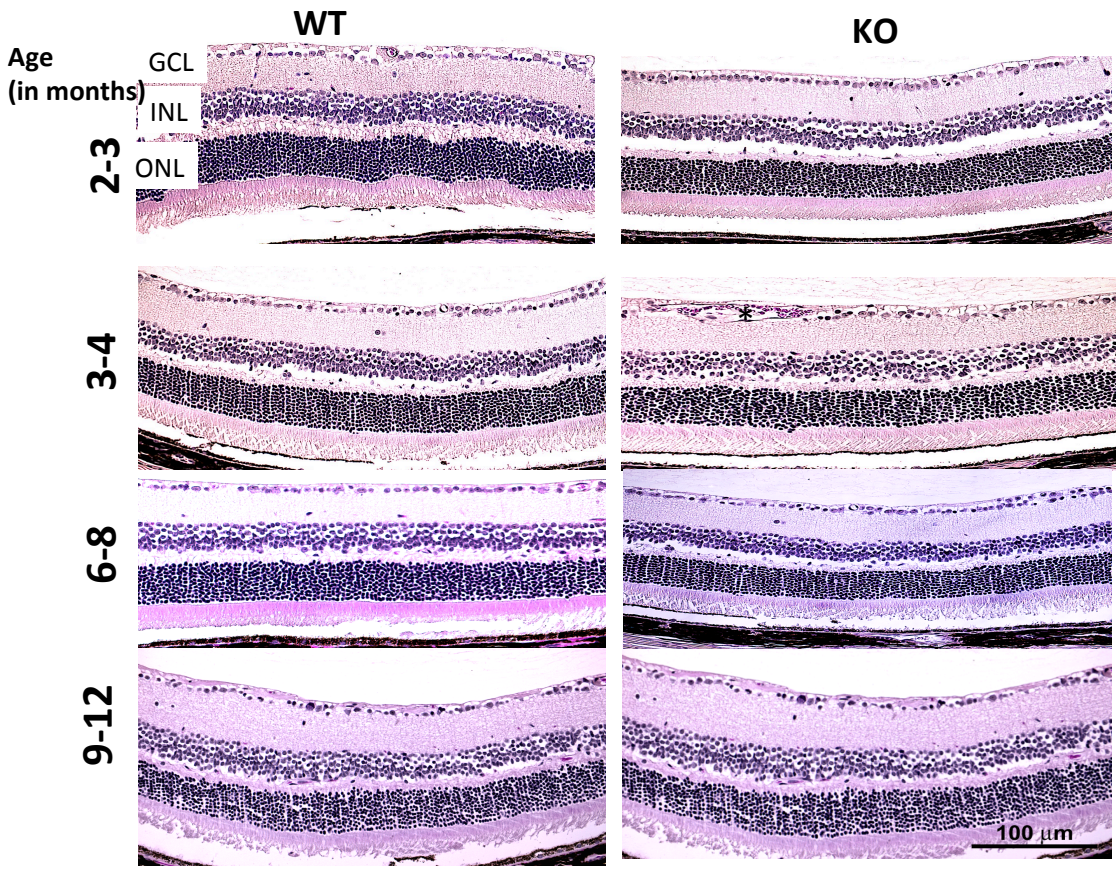

Figure 10: Retinal morphology is similar in MMP-9WT and MMP-9KO groups. At different age groups, retinal morphology between MMP-9WT and MMP-9KO groups appears similar. The asterisk (*) represents blood vessel. Abbreviations: WT= MMP-9 wild type mice, KO= MMP-9 knock out mice, GCL= ganglion cell layer, INL= inner nuclear layer and ONL= outer nuclear layer. Scale= 100 μm.

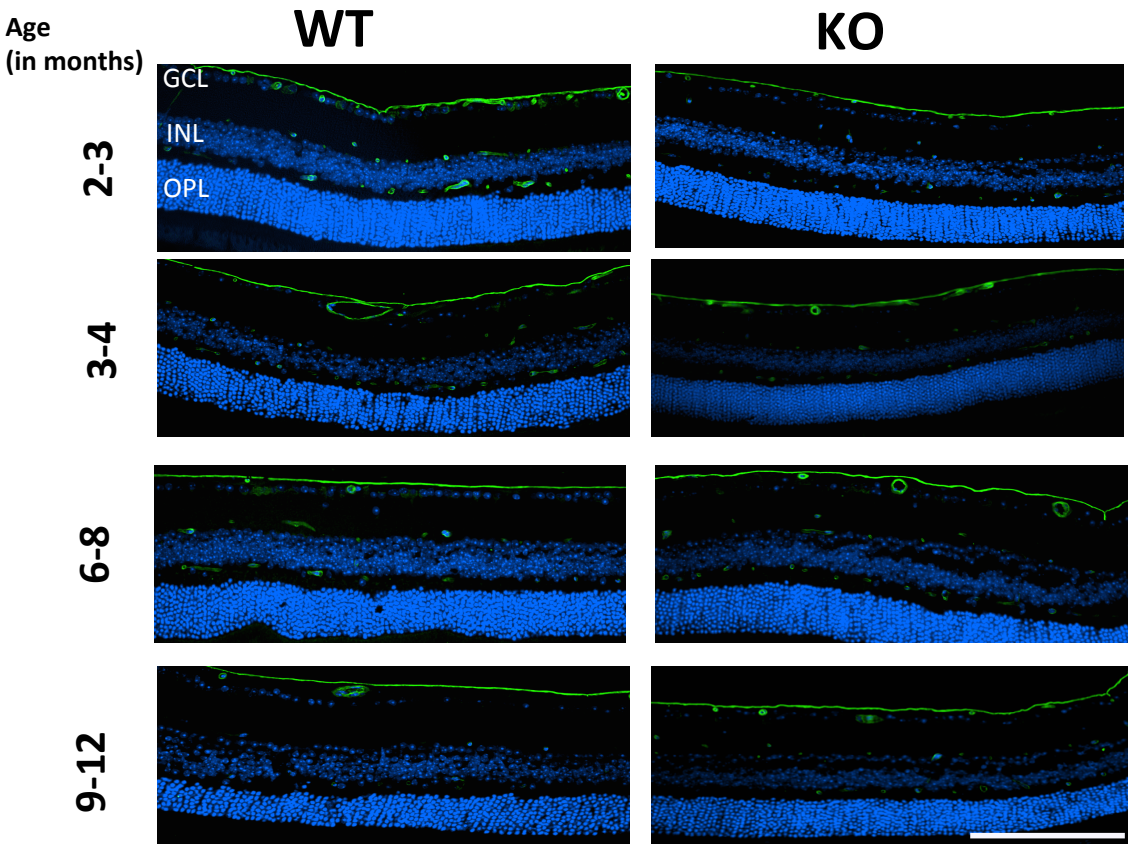

Figure 11: Laminin immunoreactivity. Laminin immunoreactivity between MMP-9WT and MMP-9KO on ocular cross-sections at 2-3, 3-4, 6-8 and 9-12 months of age. Immunoreactivity was mostly detected at the ILM with a few reactive cells in inner and outer plexiform layers. Laminin reactivity in ILM between MMP-9WT and MMP-9KO mice at different age groups was similar. Abbreviations: WT= MMP-9 wild type mice, KO= MMP-9 knock out mice, ILM= inner limiting membrane, GCL= ganglion cell layer, INL= inner nuclear layer and ONL= outer nuclear layer. Scale= 100 μm.

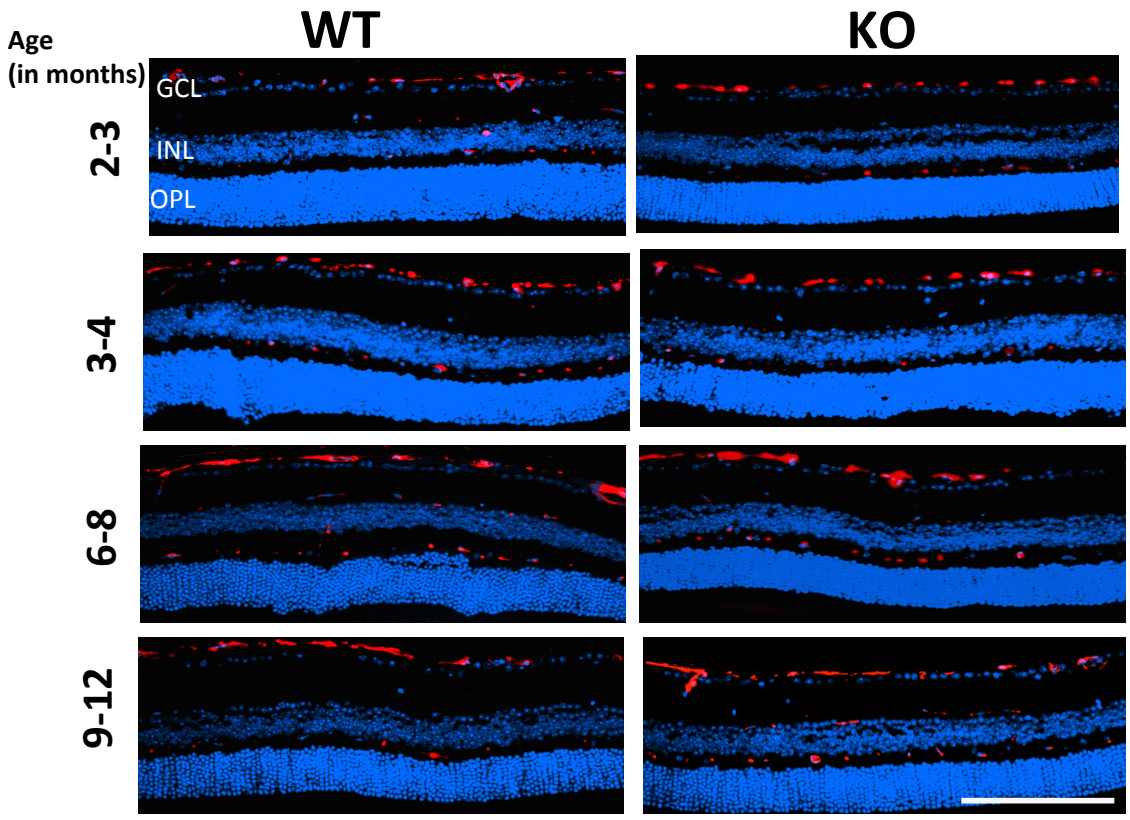

Figure 12: GFAP immunoreactivity. GFAP immunoreactivity between MMP-9WT and MMP-9KO in ocular cross-sections at 2-3, 3-4, 6-8 and 9-12 months of age. Immunoreactivity was mostly detected at the ILM with a few reactive cells in outer and inner plexiform layers. GFAP reactivity in ILM between MMP-9WT and MMP-9KO mice at different age groups was similar. Abbreviations: WT= MMP-9 wild type mice, KO= MMP-9 knock out mice, GCL= ganglion cell layer, INL= inner nuclear layer and ONL= outer nuclear layer. Scale= 100 μm.

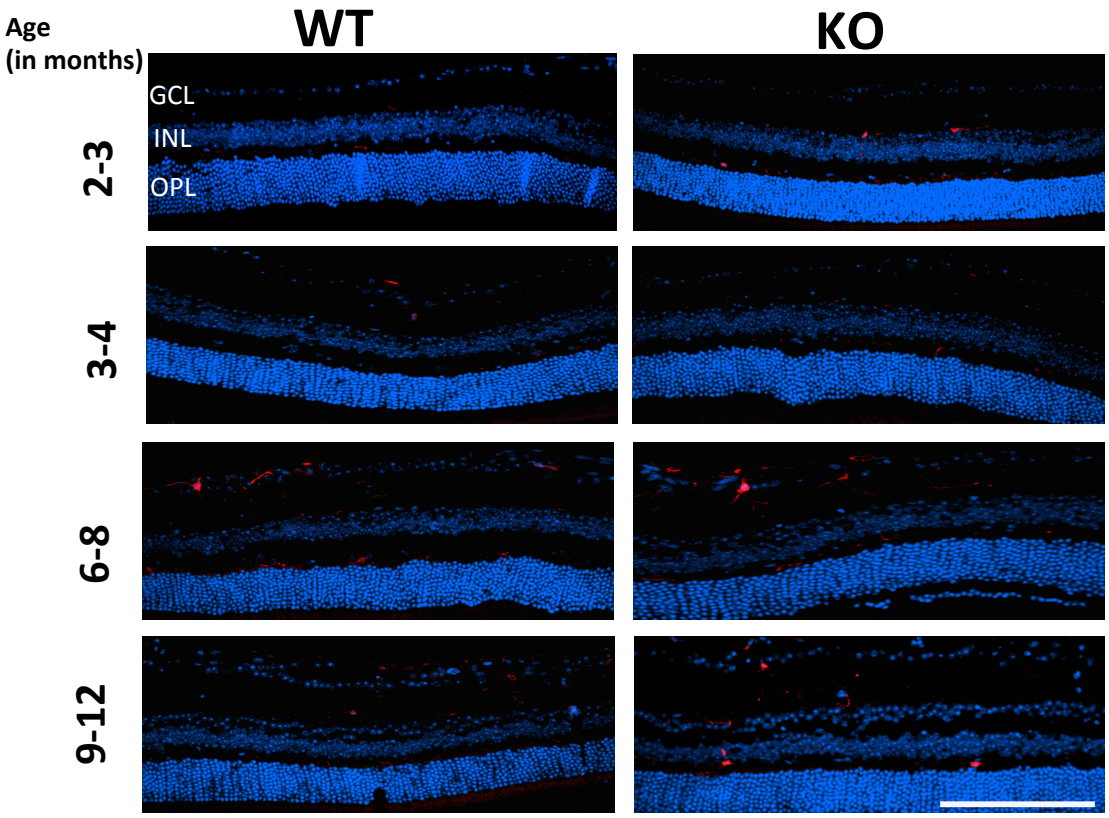

Figure 13: IBA1 immunoreactivity. Iba1 immunoreactivity between MMP-9WT and MMP-9KO in ocular cross-sections at 2-3, 3-4, 6-8 and 9-12 months of age. Iba1 localization was sparsely observed almost in all of the layers of the retina except the outer nuclear layer in both MMP-9WT and KO groups Abbreviations: WT= MMP-9 wild type mice, KO= MMP-9 knock out mice, GCL= ganglion cell layer, INL= inner nuclear layer and ONL= outer nuclear layer. Scale= 100 µm.

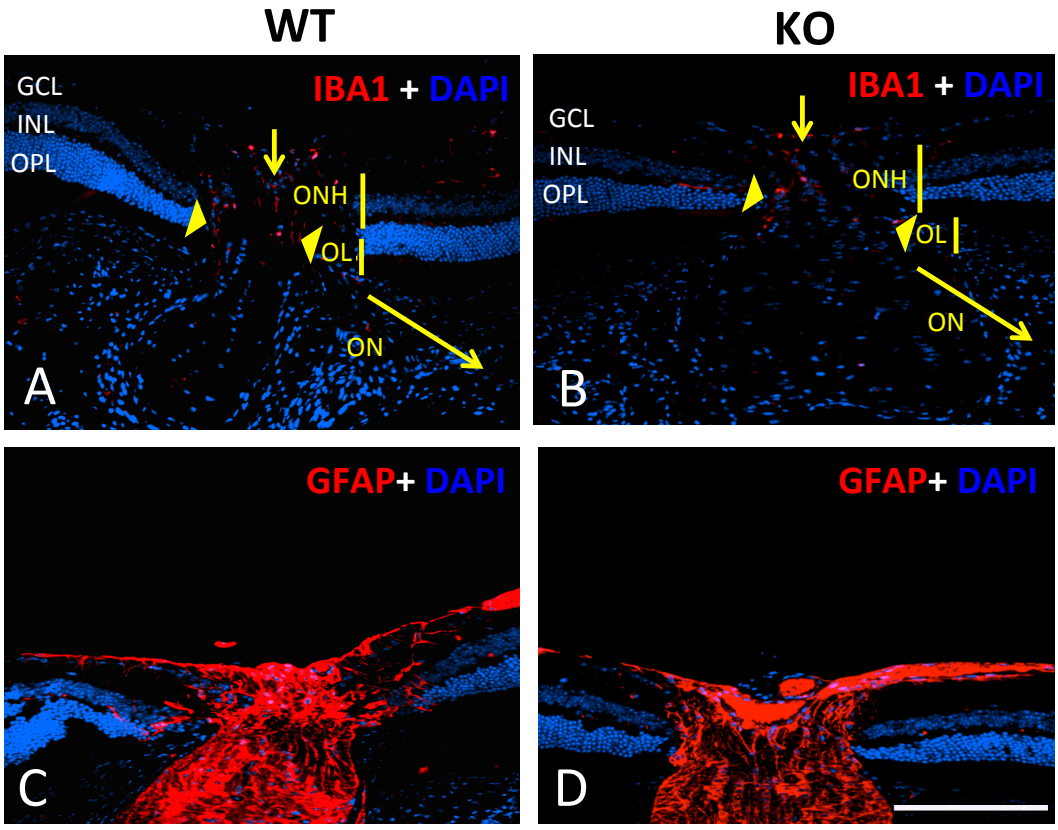

Figure 14: Iba1 and GFAP immunoreactivity in optic nerve head sections. A-B: Cross-sections across the optic nerve head (ONH), lamina (OL), and nerve (ON), reveals the compartmentalization of microglia in both MMP-9WT and MMP-9KO mice at 9-12 months of age. In ONH, microglia cluster in the innermost region of the ONH (yellow arrow) as well as in a plane across the OL (between arrowheads). C-D: Cross-sections across the optic nerve head reveal similar GFAP reactivity in both MMP-9WT and MMP-9KO mice at 9-12 months of age. Abbreviations: WT= MMP-9 wild type mice, KO= MMP-9 knock out mice, GCL= ganglion cell layer, INL= inner nuclear layer and ONL= outer nuclear layer. Scale= 100 μm.

A.

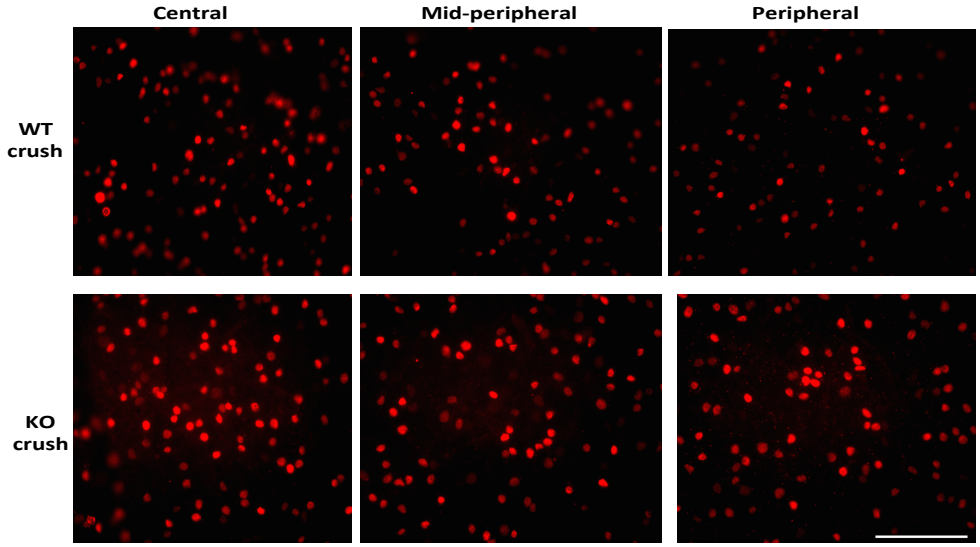

B.

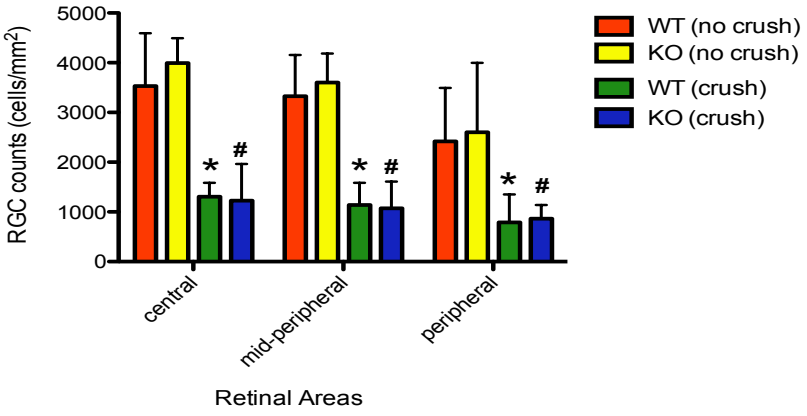

Figure 15: Brn3a+ cell count on retinal wholemounts 7 days after optic nerve crush. A: Immunofluorescence pictures from central, mid peripheral and peripheral retinal samples in MMP-9WT and MMP-9KO groups undergoing optic nerve crush. ImageJ was used to quantify the cell number between these groups. B: Quantification of Brn3a+ RGCs on different retinal areas at different age groups. * $p<0.05$ WT (crush) compared to WT (no crush), # $p<0.05$ MMP-9KO (crush) compared to MMP-9KO (no crush) signifying that the optic nerve crush led to a significant decline of RGCs in both WT and KO mice. However, no significant difference was observed between WT (crush) and KO (crush). Two-way ANOVA was used for statistical analysis followed by Tukey post-hoc multiple comparison. Bars represent mean ± 95% CI. Abbreviations: C= central retinal area, MP= mid-peripheral retinal area, P= peripheral retinal area, WT= MMP-9 wild type mice and KO= MMP-9 knock out mice. Scale= 100 µm.

REFERENCES

Agapova, O. A., Kaufman, P. L., Lucarelli, M. J., Gabelt, B. T., & Hernandez, M. R. (2003). Differential expression of matrix metalloproteinases in monkey eyes with experimental glaucoma or optic nerve transection. *Brain Res, 967*(1-2), 132-143.

Agapova, O. A., Ricard, C. S., Salvador-Silva, M., & Hernandez, M. R. (2001). Expression of matrix metalloproteinases and tissue inhibitors of metalloproteinases in human optic nerve head astrocytes. *Glia, 33*(3), 205-216. doi: Doi 10.1002/1098-1136(200103)33:3<205::Aid-Glia1019>3.0.Co;2-D

Agudo, M., Perez-Marin, M. C., Lonngren, U., Sobrado, P., Conesa, A., Canovas, I., & Vidal-Sanz, M. (2008). Time course profiling of the retinal transcriptome after optic nerve transection and optic nerve crush. *Mol Vis, 14*, 1050-1063.

Ahmed, F., Brown, K. M., Stephan, D. A., Morrison, J. C., Johnson, E. C., & Tomarev, S. I. (2004). Microarray analysis of changes in mRNA levels in the rat retina after experimental elevation of intraocular pressure. *Invest Ophthalmol Vis Sci, 45*(4), 1247-1258.

Akhter, N., Nix, M., Abdul, Y., Singh, S., & Husain, S. (2013). Delta-opioid receptors attenuate TNF-alpha-induced MMP-2 secretion from human ONH astrocytes. *Invest Ophthalmol Vis Sci, 54*(10), 6605-6611. doi: 10.1167/iovs.13-12196

Alexander, J. P., Samples, J. R., & Acott, T. S. (1998). Growth factor and cytokine modulation of trabecular meshwork matrix metalloproteinase and TIMP expression. *Current Eye Research, 17*(3), 276-285.

Alexander, J. P., Samples, J. R., Van Buskirk, E. M., & Acott, T. S. (1991). Expression of matrix metalloproteinases and inhibitor by human trabecular meshwork. *Invest Ophthalmol Vis Sci, 32*(1), 172-180.

Anderson, D. R., & Hendrickson, A. (1974). Effect of intraocular pressure on rapid axoplasmic transport in monkey optic nerve. *Invest Ophthalmol, 13*(10), 771-783.

Birkedal-Hansen, H., Moore, W. G., Bodden, M. K., Windsor, L. J., Birkedal-Hansen, B., DeCarlo, A., & Engler, J. A. (1993). Matrix metalloproteinases: a review. *Crit Rev Oral Biol Med, 4*(2), 197-250.

Bosco, A., Steele, M. R., & Vetter, M. L. (2011). Early microglia activation in a mouse model of chronic glaucoma. *J Comp Neurol, 519*(4), 599-620. doi: 10.1002/cne.22516

Bradley, J. M., Vranka, J., Colvis, C. M., Conger, D. M., Alexander, J. P., Fisk, A. S., & Acott, T. S. (1998). Effect of matrix metalloproteinases activity on outflow in perfused human organ culture. *Invest Ophthalmol Vis Sci, 39*(13), 2649-2658.

Bradley, J. M. B., Kelley, M. J., Rose, A., & Acott, T. S. (2003). Signaling pathways used in trabecular matrix metalloproteinase response to mechanical stretch. *Invest Ophthalmol Vis Sci, 44*(12), 5174-5181. doi: Doi 10.1167/Iovs.03.0213

Bradley, J. M. B., Kelley, M. J., Zhu, X. H., Anderssohn, A. M., Alexander, J. P., & Acott, T. S. (2001). Effects of mechanical stretching on trabecular matrix metalloproteinases. *Invest Ophthalmol Vis Sci, 42*(7), 1505-1513.

Chen, S. J., Lu, P., Zhang, W. F., & Lu, J. H. (2012). High myopia as a risk factor in primary open angle glaucoma. *International Journal of Ophthalmology, 5*(6), 750-753. doi: Doi 10.3980/J.Issn.2222-3959.2012.06.18

Chintala, S. K., Wang, N., Diskin, S., Mattox, C., Kagemann, L., Fini, M. E., & Schuman, J. S. (2005). Matrix metalloproteinase gelatinase B (MMP-9) is associated with leaking glaucoma filtering blebs. *Experimental Eye Research, 81*(4), 429-436. doi: Doi 10.1016/J.Exer.2005.03.001

Chintala, S. K., Zhang, X., Austin, J. S., & Fini, M. E. (2002). Deficiency in matrix metalloproteinase gelatinase B (MMP-9) protects against retinal ganglion cell death after optic nerve ligation. *J Biol Chem, 277*(49), 47461-47468. doi: 10.1074/jbc.M204824200

Cho, H. K., & Kee, C. (2014). Population-based glaucoma prevalence studies in Asians. *Survey of Ophthalmology, 59*(4), 434-447. doi: 10.1016/j.survophthal.2013.09.003

Day, A. C., Machin, D., Aung, T., Gazzard, G., Husain, R., Chew, P. T., & Foster, P. J. (2011). Central corneal thickness and glaucoma in East Asian people. *Invest Ophthalmol Vis Sci, 52*(11), 8407-8412. doi: 10.1167/iovs.11-7927

De Groef, L., Van Hove, I., Dekeyster, E., Stalmans, I., & Moons, L. (2013). MMPs in the trabecular meshwork: promising targets for future glaucoma therapies? *Invest Ophthalmol Vis Sci, 54*(12), 7756-7763. doi: 10.1167/iovs.13-13088

De Groef, L., Van Hove, I., Dekeyster, E., Stalmans, I., & Moons, L. (2014). MMPs in the neuroretina and optic nerve: modulators of glaucoma pathogenesis and repair? *Invest Ophthalmol Vis Sci, 55*(3), 1953-1964. doi: 10.1167/iovs.13-13630

De Paiva, C. S., Corrales, R. M., Villarreal, A. L., Farley, W. J., Li, D. Q., Stern, M. E., & Pflugfelder, S. C. (2006). Corticosteroid and doxycycline suppress MMP-9 and inflammatory cytokine expression, MAPK activation in the corneal epithelium in experimental dry eye. *Experimental Eye Research, 83*(3), 526-535. doi: 10.1016/j.exer.2006.02.004

De Palma, A. M., Verbeken, E., Van Aelst, I., Van den Steen, P. E., Opdenakker, G., & Neyts, J. (2008). Increased gelatinase B/matrix metalloproteinase 9 (MMP-9) activity in a murine model of acute coxsackievirus B4-induced pancreatitis. *Virology, 382*(1), 20-27. doi: 10.1016/j.virol.2008.08.046

Ding, C., Wang, P., & Tian, N. (2011). Effect of general anesthetics on IOP in elevated IOP mouse model. *Experimental Eye Research, 92*(6), 512-520. doi: 10.1016/j.exer.2011.03.016

Djafarzadeh, R., Sauter, M., Notohamiprodjo, S., Noessner, E., Goyal, P., Siess, W., & Nelson, P. J. (2012). Recombinant GPI-anchored TIMP-1 stimulates growth and migration of peritoneal mesothelial cells. *PLoS One, 7*(4), e33963. doi: 10.1371/journal.pone.0033963

Dreyer, E. B., & Lipton, S. A. (1999). New perspectives on glaucoma. *Jama-Journal of the American Medical Association, 281*(4), 306-308. doi: Doi 10.1001/Jama.281.4.306

Ebneter, A., Casson, R. J., Wood, J. P. M., & Chidlow, G. (2010). Microglial Activation in the Visual Pathway in Experimental Glaucoma: Spatiotemporal Characterization and Correlation with Axonal Injury. *Invest Ophthalmol Vis Sci, 51*(12), 6448-6460. doi: Doi 10.1167/Iovs.10-5284

Fechtner, R. D., & Weinreb, R. N. (1994). Mechanisms of Optic-Nerve Damage in Primary Open-Angle Glaucoma. *Survey of Ophthalmology, 39*(1), 23-42. doi: Doi 10.1016/S0039-6257(05)80042-6

Forrester, J. V., Dick, A.D., McMenamin, P.G. & Roberts, F. (2008). *The Eye: Basic Sciences in Practice*. Philadelphia, PA: Harcourt Publishers.

Gaasterland, D., Tanishima, T., & Kuwabara, T. (1978). Axoplasmic flow during chronic experimental glaucoma. 1. Light and electron microscopic studies of the monkey optic nervehead during development of glaucomatous cupping. *Invest Ophthalmol Vis Sci, 17*(9), 838-846.

Galindo-Romero, C., Aviles-Trigueros, M., Jimenez-Lopez, M., Valiente-Soriano, F. J., Salinas-Navarro, M., Nadal-Nicolas, F., & Agudo-Barriuso, M. (2011). Axotomy-induced retinal ganglion cell death in adult mice: quantitative and topographic time course analyses. *Experimental Eye Research, 92*(5), 377-387. doi: 10.1016/j.exer.2011.02.008

Ganesh, B. S., & Chintala, S. K. (2011). Inhibition of reactive gliosis attenuates excitotoxicity-mediated death of retinal ganglion cells. *PLoS One, 6*(3), e18305. doi: 10.1371/journal.pone.0018305

Goel, M., Picciani, R. G., Lee, R. K., & Bhattacharya, S. K. (2010). Aqueous humor dynamics: a review. *Open Ophthalmol J, 4*, 52-59. doi: 10.2174/1874364101004010052

Guo, L., Moss, S. E., Alexander, R. A., Ali, R. R., Fitzke, F. W., & Cordeiro, M. F. (2005). Retinal ganglion cell apoptosis in glaucoma is related to intraocular pressure and IOP-induced effects on extracellular matrix. *Invest Ophthalmol Vis Sci, 46*(1), 175-182. doi: Doi 10.1167/Iovs.04-0832

Haddadin, R. I., Dong-Jin, O. & Rhee, D.J. (2013). Latanoprost lowers intraocular pressure in matrix metalloproteinase 9-null mice.

Halfter, W., Dong, S., Dong, A., Eller, A. W., & Nischt, R. (2008). Origin and turnover of ECM proteins from the inner limiting membrane and vitreous body. *Eye (Lond), 22*(10), 1207-1213. doi: 10.1038/eye.2008.19

Hernandez, M. R. (2000). The optic nerve head in glaucoma: Role of astrocytes in tissue remodeling. *Progress in Retinal and Eye Research, 19*(3), 297-321. doi: Doi 10.1016/S1350-9462(99)00017-8

Inoue, T., Sasaki, H., Hosokawa, M., & Fukuda, Y. (2000). Axonal regeneration of mouse retinal ganglion cells by peripheral nerve transplantation; a quantitative study. *Restor Neurol Neurosci, 17*(1), 23-29.

Ito, D., Tanaka, K., Suzuki, S., Dembo, T., & Fukuuchi, Y. (2001). Enhanced expression of Iba1, ionized calcium-binding adapter molecule 1, after transient focal cerebral ischemia in rat brain. *Stroke, 32*(5), 1208-1215.

Ji, J. Z., Chang, P., Pennesi, M. E., Yang, Z., Zhang, J., Li, D. Q., & Gross, R. L. (2005). Effects of elevated intraocular pressure on mouse retinal ganglion cells. *Vision Research, 45*(2), 169-179. doi: Doi 10.1016/J.Visres.2004.08.008

Johnson, E. C., Jia, L. J., Cepurna, W. O., Doser, T. A., & Morrison, J. C. (2007). Global changes in optic nerve head gene expression after exposure to elevated intraocular pressure in a rat glaucoma model. *Invest Ophthalmol Vis Sci, 48*(7), 3161-3177. doi: Doi 10.1167/Iovs.06-1282

Kim, B. J., Braun, T. A., Wordinger, R. J., & Clark, A. F. (2013). Progressive morphological changes and impaired retinal function associated with temporal regulation of gene expression after retinal ischemia/reperfusion injury in mice. *Mol Neurodegener, 8*, 21. doi: 10.1186/1750-1326-8-21

Kirwan, R. P., Crean, J. K., Fenerty, C. H., Clark, A. F., & O'Brien, C. J. (2004). Effect of cyclical mechanical stretch and exogenous transforming growth factor-beta 1 on matrix metalloproteinase-2 activity in lamina cribrosa cells from the human optic nerve head. *Journal of Glaucoma, 13*(4), 327-334. doi: Doi 10.1097/00061198-200408000-00011

Kowluru, R. A., Zhong, Q., & Santos, J. M. (2012). Matrix metalloproteinases in diabetic retinopathy: potential role of MMP-9. *Expert Opin Investig Drugs, 21*(6), 797-805. doi: 10.1517/13543784.2012.681043

Kuehn, M. H., Fingert, J. H., & Kwon, Y. H. (2005). Retinal ganglion cell death in glaucoma: mechanisms and neuroprotective strategies. *Ophthalmol Clin North Am, 18*(3), 383-395, vi. doi: 10.1016/j.ohc.2005.04.002

Lens, A., Nemeth, S.C. & Ledford, J.K. (2008). *Ocular Anatomy and Physiology*. Thorofare, NJ. : Slack publishers.

Levesque, J. M. (2013). The Analysis of Brn3a and Thy1-CFP as Potential Markers of Retinal Ganglion Cells after Optic Nerve Injury in Mice. *Master's Thesis*, Dalhousie University, Halifax.

Lindsey, J. D., & Weinreb, R.N. (2002). Identification of the mouse uveoscleral outflow pathway using fluorescent dextran. *Invest Ophthalmol Vis Sci, 43*(7), 2201-2205.

Lively, G. D., Jiang, B., Hedberg-Buenz, A., Chang, B., Petersen, G. E., Wang, K., & Anderson, M. G. (2010). Genetic Dependence of Central Corneal Thickness among Inbred Strains of Mice. *Invest Ophthalmol Vis Sci, 51*(1), 160-171. doi: Doi 10.1167/Iovs.09-3429

Llobet, A., Gasull, X., & Gual, A. (2003). Understanding trabecular meshwork physiology: a key to the control of intraocular pressure? *News Physiol Sci, 18*, 205-209.

Maatta, M., Tervahartiala, T., Harju, M., Airaksinen, J., Autio-Harmainen, H., & Sorsa, T. (2005). Matrix metalloproteinases and their tissue inhibitors in aqueous humor of patients with primary open-angle glaucoma, exfoliation syndrome, and exfoliation glaucoma. *Journal of Glaucoma, 14*(1), 64-69.

Mabuchi, F., Lindsey, J. D., Aihara, M., Mackey, M. R., & Weinreb, R. N. (2004). Optic nerve damage in mice with a targeted type I collagen mutation. *Invest Ophthalmol Vis Sci, 45*(6), 1841-1845.

Manabe, S., Gu, Z. Z., & Lipton, S. A. (2005). Activation of matrix metalloproteinase-9 via neuronal nitric oxide synthase contributes to NMDA-induced retinal ganglion cell death. *Invest Ophthalmol Vis Sci, 46*(12), 4747-4753. doi: Doi 10.1167/Iovs.05-0128

Nadal-Nicolas, F. M., Jimenez-Lopez, M., Sobrado-Calvo, P., Nieto-Lopez, L., Canovas-Martinez, I., Salinas-Navarro, M., & Agudo, M. (2009). Brn3a as a Marker of Retinal Ganglion Cells: Qualitative and Quantitative Time Course Studies in Naive and Optic Nerve-Injured Retinas. *Invest Ophthalmol Vis Sci, 50*(8), 3860-3868. doi: Doi 10.1167/Iovs.08-3267

Nelson, A. R., Fingleton, B., Rothenberg, M. L., & Matrisian, L. M. (2000). Matrix metalloproteinases: biologic activity and clinical implications. *J Clin Oncol, 18*(5), 1135-1149.

Nilsson, I., Lindfors, C., Fetissov, S. O., Hokfelt, T., & Johansen, J. E. (2008). Aberrant agouti-related protein system in the hypothalamus of the anx/anx mouse is

associated with activation of microglia. *J Comp Neurol, 507*(1), 1128-1140. doi: 10.1002/cne.21599

Oh, D. J., Martin, J. L., Williams, A. J., Russell, P., Birk, D. E., & Rhee, D. J. (2006). Effect of latanoprost on the expression of matrix metalloproteinases and their tissue inhibitors in human trabecular meshwork cells. *Invest Ophthalmol Vis Sci, 47*(9), 3887-3895. doi: Doi 10.1167/Iovs.06-0036

Parshley, D. E., Bradley, J. M., Fisk, A., Hadaegh, A., Samples, J. R., Van Buskirk, E. M., & Acott, T. S. (1996). Laser trabeculoplasty induces stromelysin expression by trabecular juxtacanalicular cells. *Invest Ophthalmol Vis Sci, 37*(5), 795-804.

Pena, J. D. O., Agapova, O., Gabelt, B. A. T., Levin, L. A., Lucarelli, M. J., Kaufman, P. L., & Hernandez, M. R. (2001). Increased elastin expression in astrocytes of the lamina cribrosa in response to elevated intraocular pressure. *Invest Ophthalmol Vis Sci, 42*(10), 2303-2314.

Purves, D., Augustine, G.J., Fitzpatrick, D., Hall, W.C., LaMantia, A., & White, L.E. . (2012). *Neurosciences* (5th ed.). Sunderland, MA. : Sinauer Associates, Inc.

Quigley, H. A., & Addicks, E. M. (1980). Chronic experimental glaucoma in primates. II. Effect of extended intraocular pressure elevation on optic nerve head and axonal transport. *Invest Ophthalmol Vis Sci, 19*(2), 137-152.

Quigley, H. A., & Broman, A. T. (2006). The number of people with glaucoma worldwide in 2010 and 2020. *Br J Ophthalmol, 90*(3), 262-267. doi: 10.1136/bjo.2005.081224

Quigley, H. A., McKinnon, S. J., Zack, D. J., Pease, M. E., Kerrigan-Baumrind, L. A., Kerrigan, D. F., & Mitchell, R. S. (2000). Retrograde axonal transport of BDNF in retinal ganglion cells is blocked by acute IOP elevation in rats. *Invest Ophthalmol Vis Sci, 41*(11), 3460-3466.

Quigley, H. A., Nickells, R. W., Kerrigan, L. A., Pease, M. E., Thibault, D. J., & Zack, D. J. (1995). Retinal Ganglion-Cell Death in Experimental Glaucoma and after Axotomy Occurs by Apoptosis. *Invest Ophthalmol Vis Sci, 36*(5), 774-786.

Quina, L. A., Pak, W., Lanier, J., Banwait, P., Gratwick, K., Liu, Y., & Turner, E. E. (2005). Brn3a-expressing retinal ganglion cells project specifically to thalamocortical and collicular visual pathways. *J Neurosci, 25*(50), 11595-11604. doi: 10.1523/JNEUROSCI.2837-05.2005

Resta, V., Novelli, E., Vozzi, G., Scarpa, C., Caleo, M., Ahluwalia, A., & Galli-Resta, L. (2007). Acute retinal ganglion cell injury caused by intraocular pressure spikes is mediated by endogenous extracellular ATP. *European Journal of Neuroscience, 25*(9), 2741-2754. doi: Doi 10.1111/J.1460-9568.2007.05528.X

Robertson, J. V., Siwakoti, A., & West-Mays, J. A. (2013). Altered expression of transforming growth factor beta 1 and matrix metalloproteinase-9 results in elevated intraocular pressure in mice. *Mol Vis, 19*, 684-695.

Rönkkö, S., Rekonen, P., Kaarniranta, K., Puustjärvi, T., Teräsvirta, M., & Uusitalo, H. (2007). Matrix metalloproteinases and their inhibitors in the chamber angle of normal eyes and patients with primary open-angle glaucoma and exfoliation glaucoma. *Graefe's archive for clinical and experimental ophthalmology, 245*(5), 697-704.

Schlotzer-Schrehardt. (2002). Matrix Metalloproteinases and Their Inhibitors in Aqueous Humor of Patients with Pseudoexfoliation Syndrome/Glaucoma and Primary Open-Angle Glaucoma. *Invest Ophthalmol Vis Sci, 44*(3), 117.

Sivak, J. M., & Fini, M. E. (2002). MMPs in the eye: emerging roles for matrix metalloproteinases in ocular physiology. *Progress in Retinal and Eye Research, 21*(1), 1-14.

Smith, S. (2008). *Basic ocular anatomy* (Vol. 3).

Sommer, A., Tielsch, J. M., Katz, J., Quigley, H. A., Gottsch, J. D., Javitt, J., & Singh, K. (1991). Relationship between Intraocular-Pressure and Primary Open Angle Glaucoma among White and Black-Americans - the Baltimore Eye Survey. *Arch Ophthalmol, 109*(8), 1090-1095.

Song, B. J., & Caprioli, J. (2014). New directions in the treatment of normal tension glaucoma. *Indian J Ophthalmol, 62*(5), 529-537. doi: 10.4103/0301-4738.133481

Sun, M. H., Chen, K. J., Tsao, Y. P., Kao, L. Y., Han, W. H., Lin, K. K., & Pang, J. H. (2011). Down-regulation of matrix metalloproteinase-9 by pyrrolidine dithiocarbamate prevented retinal ganglion cell death after transection of optic nerve in rats. *Current Eye Research, 36*(11), 1053-1063. doi: 10.3109/02713683.2011.606591

Tektas, O. Y., & Lutjen-Drecoll, E. (2009). Structural changes of the trabecular meshwork in different kinds of glaucoma. *Experimental Eye Research, 88*(4), 769-775. doi: 10.1016/j.exer.2008.11.025

Tezel, G. (2011). The immune response in glaucoma: A perspective on the roles of oxidative stress. *Experimental Eye Research, 93*(2), 178-186. doi: Doi 10.1016/J.Exer.2010.07.009

Tsuruga, H., Murata, H., Araie, M., & Aihara, M. (2012). A model for the easy assessment of pressure-dependent damage to retinal ganglion cells using cyan fluorescent protein-expressing transgenic mice. *Mol Vis, 18*, 2468-2478.

Vass, C., Hirn, C., Sycha, T., Findl, O., Bauer, P., & Schmetterer, L. (2007). Medical interventions for primary open angle glaucoma and ocular hypertension. *Cochrane Database Syst Rev*(4), CD003167. doi: 10.1002/14651858.CD003167.pub3

Vermeer, P. D., Denker, J., Estin, M., Moninger, T. O., Keshavjee, S., Karp, P., & Zabner, J. (2009). MMP9 modulates tight junction integrity and cell viability in human airway epithelia. *Am J Physiol Lung Cell Mol Physiol, 296*(5), L751-762. doi: 10.1152/ajplung.90578.2008

Vittitow, J., & Borras, T. (2004). Genes expressed in the human trabecular meshwork during pressure-induced homeostatic response. *Journal of Cellular Physiology, 201*(1), 126-137. doi: Doi 10.1002/Jcp.20030

Vu, T. H., Shipley, J. M., Bergers, G., Berger, J. E., Helms, J. A., Hanahan, D., & Werb, Z. (1998). MMP-9/gelatinase B is a key regulator of growth plate angiogenesis and apoptosis of hypertrophic chondrocytes. *Cell, 93*(3), 411-422. doi: Doi 10.1016/S0092-8674(00)81169-1

Vu, T. H., & Werb, Z. (2000). Matrix metalloproteinases: effectors of development and normal physiology. *Genes Dev, 14*(17), 2123-2133.

Wang, S. W., Mu, X., Bowers, W. J., Kim, D. S., Plas, D. J., Crair, M. C., & Klein, W. H. (2002). Brn3b/Brn3c double knockout mice reveal an unsuspected role for Brn3c in retinal ganglion cell axon outgrowth. *Development, 129*(2), 467-477.

Weinreb, R. N., & Khaw, P. T. (2004). Primary open-angle glaucoma. *Lancet, 363*(9422), 1711-1720. doi: Doi 10.1016/S0140-6736(04)16257-0

Weinstein, W. L., Dietrich, U. M., Sapienza, J. S., Carmichael, K. P., Moore, P. A., & Krunkosky, T. M. (2007). Identification of ocular matrix metalloproteinases present within the aqueous humor and iridocorneal drainage angle tissue of normal and glaucomatous canine eyes. *Veterinary Ophthalmology, 10*, 108-116. doi: Doi 10.1111/J.1463-5224.2007.00586.X

West-Mays, J. A., & Pino, G. (2008). Matrix Metalloproteinases as Mediators of Primary and Secondary Cataracts. *Expert Review in Ophthalmology, 2*(6), 931-938.

Williams, R. W., Strom, R. C., Rice, D. S., & Goldowitz, D. (1996). Genetic and environmental control of variation in retinal ganglion cell number in mice. *J Neurosci, 16*(22), 7193-7205.

Woodword, D. F. G., DW. (2004). The inflow and outflow of anti-glaucoma drugs. *Trends in Pharmacological Science, 25*(5), 238-241.

WuDunn, D. (2001). The effect of mechanical strain on matrix metalloproteinase production by bovine trabecular meshwork cells. *Current Eye Research, 22*(5), 394-397. doi: Doi 10.1076/Ceyr.22.5.394.5500

Zhang, X., Cheng, M., & Chintala, S. K. (2004a). Kainic acid-mediated upregulation of matrix metalloproteinase-9 promotes retinal degeneration. *Invest Ophthalmol Vis Sci, 45*(7), 2374-2383.

Zhang, X., Cheng, M., & Chintala, S. K. (2004b). Optic nerve ligation leads to astrocyte-associated matrix metalloproteinase-9 induction in the mouse retina. *Neurosci Lett, 356*(2), 140-144.

Zhang, X., & Chintala, S. K. (2004). Influence of interleukin-1 beta induction and mitogen-activated protein kinase phosphorylation on optic nerve ligation-induced matrix metalloproteinase-9 activation in the retina. *Experimental Eye Research, 78*(4), 849-860. doi: 10.1016/j.exer.2003.10.018

Zhang, X., Sakamoto, T., Hata, Y., Kubota, T., Hisatomi, T., Murata, H., & Inomata, H. (2002). Expression of matrix metalloproteinases and their inhibitors in experimental retinal ischemia-reperfusion injury in rats. *Experimental Eye Research, 74*(5), 577-584. doi: Doi 10.1006/Exer.2001.1152

APPENDIX
COPYRIGHT PERMISSION

SINAUER ASSOCIATES, Inc. • Publishers • P.O. Box 407, 23 Plumtree Rd. • Sunderland, MA 01375

Telephone: (413) 549-4300
Fax: (413) 549-1118
Email: permissions@sinauer.com

PERMISSIONS AGREEMENT

August 7, 2014

Permission granted to:
Anuja Siwakoti
1280 Main Street West
Hamilton, ON
CANADA L8S 4L8

Email: siwakoa@mcmaster.ca

Material to be reproduced:
Purves et al: *Neuroscience, Fifth Edition*
Figure 11.5 B, page 236

To be reproduced in the work:
Anuja Siwakoti's MS Thesis entitled "Consequence of MMP-9 deficiency on intraocular pressure regulation and retinal ganglion cell survival" to be published by McMaster University

Sinauer Associates owns copyright to the material described above and hereby grants permission for the one-time use of the material as specified, and for nonexclusive world rights provided that full and appropriate credit is given to the original source and that the work is for NON-COMMERCIAL use only. Please request permission for further use in subsequent editions, translations, or revisions of the work.

[redacted]
Sherri L. Ellsworth
Permissions Coordinator

August 7, 2014
Date

Please acknowledge your acceptance of these terms by signing one copy of this form and returning it to Sinauer Associates. Permission Agreement is not valid until signed by applicant and received by Sinauer Associates.

[redacted]
Signature of Applicant

August 7, 2014
Date